# Understanding the Impacts of Limited Channel State Information on Massive MIMO Cellular Network Optimization

Jia Liu, *Senior Member, IEEE,* Atilla Eryilmaz,, *Senior Member, IEEE,* Ness B. Shroff, *Fellow, IEEE,* Elizabeth S. Bentley, *Member, IEEE*

***Abstract*—To support the multi-Gigabit per second data rates of 5G wireless networks, there have been significant efforts on the research and development of Massive MIMO (M-MIMO) technologies at the physical layer. So far, however, the understanding of how M-MIMO could affect the performance of network control and optimization algorithms remains rather limited. In this paper, we focus on analyzing the performance of the queue-length-based joint congestion control and scheduling framework (QCS) over M-MIMO cellular networks with limited channel state information (CSI). Our contributions in this paper are two-fold: i) We characterize the scaling performance of the queue-lengths and show that there exists a phase transitioning phenomenon in the steady-state queue-length deviation with respect to the CSI quality (reflected in the number of bits $B$ that represent CSI); and ii) We characterize the congestion control rate scaling performance and show that there also exists a phase transitioning phenomenon in steady-state congestion control rate deviation respect to the CSI quality. Collectively, the findings in this paper advance our understanding of the trade-offs between delay, throughput, and the accuracy/complexity of CSI acquisition in M-MIMO cellular network systems.**

***Index Terms*—Massive MIMO, channel state information, throughput-delay trade-off, network utility optimization.**

## I. Introduction

To allow 5G wireless networks to support multi-Gigabit per second data rates, there have been significant recent efforts on the research and development of massive multiple-input multiple-output systems, or simply being referred to as Massive MIMO (M-MIMO). In contrast to conventional multi-antenna technologies, the number of antennas in M-MIMO is on the order of hundreds or even thousands. Also, in another key 5G technology called millimeter-wave (mmWave) communication, one can easily pack a large antenna array into small form factors thanks to the short wavelengths, leading to a perfect marriage between M-MIMO and mmWave communications. To date, various promising theoretical results on M-MIMO capacity gain and transmit power efficiency have been established (see, e.g., [1]–[3] for comprehensive overviews). Also, some lab-scale M-MIMO prototypes have been built and favorable field test results have been reported (e.g., [4], [5]). However, in spite of all of this progress, the existing research efforts on M-MIMO are mostly concerned with problems at the physical layer or signal processing aspects. The understanding of how M-MIMO could affect the performance of network control, scheduling, and resource allocation algorithms remains limited in the literature. In this paper, our goal is to fill this gap by conducting an in-depth theoretical study on the interactions between M-MIMO physical layer and network control and optimization algorithms at higher layers, as well as their impacts on queueing delay and throughput performances.

To this end, in this paper, we focus on the performance analysis of the celebrated queue-length-based congestion control and scheduling framework (QCS) (see, e.g., [6]–[9], and [10] for a survey) in M-MIMO-based cellular systems, where the M-MIMO data transmissions can rely only on *limited channel state information* (CSI). The fundamental rationale of our work is that, as noted by many researchers [1], [2], CSI acquisition has become one of the most fundamental limiting factors in the design of M-MIMO-based cellular systems. Generally speaking, to leverage the MIMO spatial multiplexing benefits, the transmitter must obtain CSI to perform spatial beamforming so that independent data streams can be simultaneously transmitted. In conventional MIMO-based networks, such CSI is usually learned at each mobile station based on pilot symbols and fed back to the base station (BS). However, due to the constraints on feedback channel capacity and channel coherence time, this traditional CSI feedback approach scales poorly with the increase of antennas in M-MIMO. An alternative CSI acquisition strategy is to let the system operate in time-division duplexing mode and, based on channel reciprocity, use the uplink CSI measured at the BS for downlink transmissions. However, the uplink CSI accuracy could still be limited in practice due to multiple reasons: 1)

Manuscript received December 15, 2016 and revised May 1, 2017. This work is supported by NSF grants CCF 1618318, CNS 1527078, 1446582, 1314538, 1518829, 1421576, WiFiUS 1456806, CMMI 1562065, ECCS 1444026; ONR grant N00014-15-1-2166; ARO grant W911NF-14-1-0368; DTRA grants HDTRA 1-14-1-0058, 1-15-1-0003, AFRL VFRP and SFFP awards; DARPA grant HROOll-15-C-0097, and QNRF grant NPRP 7-923-2-344. This paper was presented in part at ACM MobiHoc'16, Paderborn, Germany, July 2016.

Jia Liu, Atilla Eryilmaz, and Ness B. Shroff are with the Department of Electrical and Computer Engineering, The Ohio State University, Columbus, OH, 43210 USA (e-mail: {liu.1736, eryilmaz.2, shroff.11}@osu.edu).

Elizabeth S. Bentley is with the Air Force Research Laboratory, Information Directorate, Rome, NY, 13441 USA (e-mail: elizabeth.bentley.3@us.af.mil).

DISTRIBUTION STATEMENT A: Approved for Public Release; distribution unlimited 88ABW-2017-1861 on 19 April 2017. ACKNOWLEDGMENT OF SUPPORT AND DISCLAIMER (a) Contractor acknowledges Government's support in the publication of this paper. This material is based upon work funded by AFRL under AFRL Contract No. FA8750-16-3-6003. (b) Any opinions, findings and conclusions or recommendations expressed in this material are those of the author(s) and do not necessarily reflect the views of AFRL.

Digital Object Identifier xx.xxxx/XXXX.xxxx.xxxxx.

As indicated in the original Introduction, it has been observed in [1], [11] that the channel reciprocity assumption may not perfectly hold in practice due to the magnetic properties of the channel environment and transceiver hardware chains; 2) In millimeter-wave (mmWave) Massive MIMO systems (where a large number of antennas can be easily packed into a small form factor due to the short wavelength), the channel coherence time is around an order of magnitude lower than that of microwave bands since Doppler shifts scale linearly with frequencies. This short channel coherence time implies that uplink CSI estimation in mmWave Massive MIMO systems is challenging; 3) Due to the limited transmit power at the mobile station and the lack of beamforming gains for uplink pilot symbols, the accuracy of TDD-based CSI estimation through channel reciprocity is limited.

In this paper, we accept the reality that CSI inaccuracy is unavoidable and we do not require full CSI at the M-MIMO BS. Instead, we assume that the CSI at the BS is limited and accurate only to a certain degree. Such limited CSI can be obtained by a small amount of feedback from each mobile device using a limited number of bits to approximately represent its channel instantiation. Alternatively, the BS could approximately measure the downlink CSI based on the channel reciprocity assumption. In such cases, one interesting question naturally arises: *How does the limited CSI affect the performance of the QCS framework?* In particular, it is well-known that the QCS framework is throughput-optimal under full CSI and achieves an $[O(1/K), O(K)]$ utility-delay trade-off, where $K > 0$ is a system parameter [8]. Also, the average queue-length deviation and the congestion control rate optimality gap scale as $O(\sqrt{K})$ [12] and $O(1/\sqrt{K})$ [7], respectively. However, when the QCS framework is adopted in M-MIMO cellular networks with limited CSI, it begs the following question: *Will the same utility and delay performance scaling laws continue to hold?* As will be seen later, due to the complex cross-layer interactions (e.g., precoder design, choice of channel quantization codebook, power allocations, etc.) in M-MIMO cellular systems, answering this question is challenging.

The main contribution of this paper is that we theoretically characterize the queueing delay and network utility-optimality performance of the QCS framework in M-MIMO cellular networks with $B$-bit limited CSI. Our main results and technical contributions are as follows:

- We show that the queues in the network remain stable under QCS under imperfect CSI; and the steady-state average queue-lengths still follow an $O(K)$ linear scaling. For an imperfect CSI scheme is accurate up to the $B$ most significant bit, the slope (i.e., the hidden constant in Big-O) is affected by $B$: The larger the value of $B$ (more accurate CSI), the more gradual the slope becomes. Moreover, the steady-state queue-length deviation from the mean exhibits a phase transition phenomenon: There exists a critical value $B_{\rm cr}$ such that: i) For all $0 < B < B_{\rm cr}$, the steady-state queue-length deviation is bounded by $O(D_{(B)}K)$, where $D_{(B)} > 0$ is a quantity that depends on the specific channel quantization codebook design; and ii) For all $B \geq B_{\rm cr}$, the steady-state queue-length deviation scales as $O(\sqrt{K})$, i.e., recovering the same scaling law under full CSI.
- For any given $B$-bit limited CSI collection scheme, we show that the steady-state average congestion control rates under the QCS framework increase as $B$ increases. Interestingly, the same phase transition phenomenon also happens in the congestion control rates in the following sense: There exists the same critical value $B_{\rm cr}$ such that: i) For all $0 < B < B_{\rm cr}$, the steady-state congestion control rate deviation scales as $O(D_{(B)})$ and independent of $K$; and ii) For all $B \geq B_{\rm cr}$, the steady-state congestion control deviation scales as $O(1/\sqrt{K})$, also recovering the same scaling law under the full CSI.
- Collectively, all queue-length and congestion control rate scaling results and their phase transition effects advance our understanding of the trade-offs between delay, throughput, and the accuracy/complexity of CSI acquisition. Also, our results suggest that delay and throughput scalings could potentially be employed as useful proxies to control CSI quality and acquisition complexity in M-MIMO networks. More importantly, our work establishes a unifying theoretical framework as well as design guidelines in practice that enable the development of effective CSI quantization schemes for M-MIMO cellular networks.

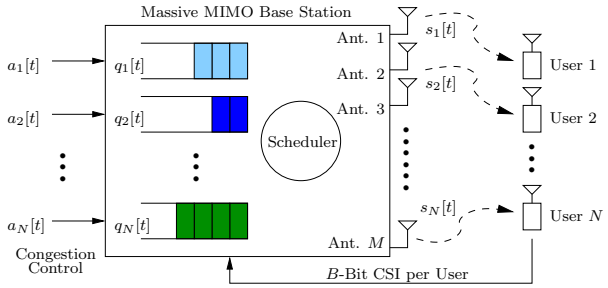


Fig. 1. A Massive MIMO cellular downlink with $M$ antennas and $N$ users, with $M \gg N$.

The remainder of this paper is organized as follows: In Section II, we introduce network model and the problem formulation. In Section III, we introduce the queue-length-based congestion control and scheduling framework and present the main results of this work. Section IV presents the numerical results and Section V concludes this paper.

## II. Network Model and Problem Formulation

**Notation:** We use boldface to denote matrices/vectors. We let $\mathbf{A}^\top$ and $\mathbf{A}^\dagger$ denote the transpose and conjugate transpose of $\mathbf{A}$, respectively. We let $\mathbf{v}_1 \geq \mathbf{v}_2$ denote entry-wise inequality between vectors. We let $v_m$ represent the $m$-th entry of vector $\mathbf{v}$. We use $\|\cdot\|$ and $\|\cdot\|_1$ to denote $L^2$- and $L^1$-norms, respectively. We use $\mathbb{R}$, $\mathbb{C}$, and $\mathbb{Z}$ to denote real, complex, and integer spaces, respectively.

**1) Massive MIMO Downlink Channel:** As shown in Fig. 1, we consider an M-MIMO cellular downlink system, where the BS has $M$ antennas and serves $N$ simultaneously active single-antenna users. In this paper, we focus on the cases where $M \gg N$ (e.g., $M$ is in hundreds or even thousands, while $N$ could be well less than tens). Thanks to such excess

degrees of freedom at the BS, it is possible for the BS to serve all $N$ users by simultaneously forming $N$ spatial beams. We note that the number of users in a cell usually exceed the number of antennas. However, the number of simultaneously active users could be less than the number of antennas in a Massive MIMO system, especially in small cells (a key feature in 5G mmWave M-MIMO wireless networks) and non-peak hours. In fact, exploiting the small number of simultaneously active users is the foundation of most statistical multiplexing schemes. In this paper, we focus on the case where the number of users is less than the number of antennas and the associated RF chains, so that the system can afford to serve all users simultaneously. This would allow us to first simplify the problem and fully understand the effects of *imperfect CSI* (caused by numerous factors as outlined in Sec. I) in Massive MIMO cellular systems.

We assume that the system operates under a time-slotted fashion and time is indexed by $t \in \{0, 1, 2, \ldots\}$. We let $\mathbf{H}[t] \in \mathbb{C}^{N\times M}$ denote the channel gain matrix in time-slot $t$ between the BS and the users. We assume independent quasi-static block fading, i.e., each entry in $\mathbf{H}[t]$ is constant in one time-slot and independently varies in the next time-slot. Moreover, one important property of M-MIMO channels with $M \gg N$ is that, under favorable propagation conditions, the row vectors of $\mathbf{H}[t]$ are asymptotically orthogonal as $M \to \infty$ [2]. This property enables the use of simple matched-filter (MF) beamforming strategy to approach the MIMO broadcast channels [2][1]. Thus, in what follows, we will briefly introduce some related preliminaries of MF beamforming for M-MIMO.

**2) Matched-Filter Beamforming:** For the M-MIMO cellular downlink in Fig. 1, the received signal of user $n$ in time-slot $t$ can be written as: $y_n[t] = x_n[t]\sqrt{p_n[t]}\mathbf{h}_n^\dagger[t]\mathbf{w}_n[t] + \sum_{j=1,\neq n}^{N} x_j[t]\sqrt{p_j[t]}\mathbf{h}_n^\dagger[t]\mathbf{w}_j[t] + v_n[t]$, where $\mathbf{h}_n[t] \in \mathbb{C}^M$ is the channel gain vector seen at user $n$ in time-slot $t$, i.e., the $n$-th row in $\mathbf{H}[t]$; $p_n[t]$ is the power allocated to user $n$ in time-slot $t$; $x_n[t]$ represents a unit-power data symbol intended for user $n$ in time-slot $t$; $\mathbf{w}_n[t] \in \mathbb{C}^N$ is a unit-norm linear precoding vector for user $n$ in time-slot $t$; and $v_n[t]$ is the white complex Gaussian noise at user $n$ in time-slot $t$ with power $N_0$. Under MF beamforming, one simply let $\mathbf{w}_n[t] = \mathbf{h}_n[t]$, i.e., the $n$-th row in $\mathbf{H}[t]$. In this setting, the achievable rate under MF beamforming can be computed as:

$$r_n[t] = \log_2\left(1 + \frac{p_n[t]|\mathbf{h}_n^\dagger[t]\mathbf{w}_n[t]|^2}{N_0 + \sum_{j=1,\neq n}^{N} p_j[t]|\mathbf{h}_n^\dagger[t]\mathbf{w}_j[t]|^2}\right) \overset{(a)}{\approx} \log_2\left(1 + \frac{p_n[t]}{N_0}\|\mathbf{h}_n[t]\|^2\right), \quad (1)$$

where $(a)$ follows from the fact that the rows of $\mathbf{H}[t]$ in M-MIMO channels are nearly orthogonal, i.e., $\mathbf{h}_n^\dagger[t]\mathbf{w}_j[t] = \mathbf{h}_n^\dagger[t]\mathbf{h}_j[t] \approx 0$, $\forall n \neq j$, when $M$ is sufficiently large.

We assume that the channel fading can be characterized by a total of $F$ states $\mathbf{H}^{(1)}, \ldots, \mathbf{H}^{(F)}$, where each $\mathbf{H}^{(f)} \in \mathbb{C}^{N\times M}$, $f = 1, \ldots, F$, corresponds to the channel qualities between the $M$ antennas and $N$ users in state $f$. For each $\mathbf{H}^{(f)}$, we let $\mathcal{C}_{\mathbf{H}^{(f)}}$ denote the achievable MF rate region, which is the convex hull of all achievable MF rate vectors in state $f$ under all feasible power allocations:

$$\mathcal{C}_{\mathbf{H}^{(f)}} \triangleq \mathrm{CH}\left\{ r_n^{(f)}, 1 \le n \le N \;\middle|\; \begin{array}{l} r_n^{(f)} = \log_2\left(1 + \frac{p_n}{N_0}\|\mathbf{h}_n^{(f)}\|^2\right) \\ p_n \ge 0, \forall n, \sum_{n=1}^{N} p_n \le P_{\max} \end{array} \right\},$$

where $\mathrm{CH}\{\cdot\}$ represents the convex hull operation, $p_n$ denotes the power allocated of user $n$, and $P_{\max}$ denotes the maximum transmission power at the BS. Clearly, due to the maximum power constraint, there exists an $r_{\max} < \infty$ such that $r_n^{(f)} \le r^{\max}$, $\forall n, f$. We let $\mathbf{r}^{(f)} = [r_1^{(f)}, \ldots, r_N^{(f)}]^\top \in \mathbb{R}^N$ denote the feasible MF rates in state $f$. We let $\pi_f \triangleq \Pr\{\mathbf{H}[t] = \mathbf{H}^{(f)}\}$ be the stationary distribution of the channel state process being in state $f$. We let $\bar{\mathcal{C}}$ denote the mean MF achievable rate region, which can be written as:

$$\bar{\mathcal{C}} \triangleq \left\{ \mathbf{r} \;\middle|\; \mathbf{r} = \sum_{f=1}^{F} \pi_f \mathbf{r}^{(f)},\ \forall \mathbf{r}^{(f)} \in \mathcal{C}_{\mathbf{H}^{(f)}} \right\}. \quad (2)$$

We note that, in this paper, neither the channel state statistics nor $\bar{\mathcal{C}}$ is assumed to be known at the BS under the QCS algorithm, which will be introduced in Section III.

**3) $B$-Bit Limited CSI:** The use of MF beamforming (i.e., $\mathbf{w}_n[t] = \mathbf{h}_n[t]$) means that the BS requires full CSI $\mathbf{H}[t]$, $\forall t$. However, as mentioned in Section I, it becomes increasingly difficult to acquire full CSI as $M$ gets large. One way to address this challenge is to use limited CSI by quantizing the channel (e.g., [14]–[18]). As shown in Fig. 1, such limited CSI can be obtained from a small amount of feedback by each user using a small number of bits to represent a quantized channel state, which is accurate up to the $B$ most significant bits. Note that in the M-MIMO and millimeter-wave (mmWave) systems literature, some hybrid beamforming/precoding architecture has been proposed for frequency division duplex (FDD) systems with a reduced number of RF chains and reduced CSI feedback based on second-order statistics of the channel vectors, i.e., the channel covariance matrices (see, e.g., [19], [20]). In these hybrid beamforming systems, due to the time spent on analog beamforming, the time used for estimating the effective channel CSI for digital beamforming is further reduced, although the dimension of the effective channels is reduced. This reduced estimation time in effective channel also introduce inaccuracy in effective channel CSI.

Alternatively, in time-division duplex (TDD) mode, Fig. 1 represents that the BS measures the uplink CSI, which is accurate up to the $B$ most significant bits and will be used for downlink transmissions[2]. In both cases, the value of $B$ can

[1]For MIMO broadcast channels, it is known that dirty paper coding (DPC) is capacity-achieving [13]. However, DPC is a nonlinear precoding scheme that is difficult to implement. In contrast, the capacity loss of the simple MF compared to DPC is negligible in the high signal-to-noise ratio regime [2].

[2]Under the TDD mode, there is no need for quantized CSI feedback. However, uplink CSI inaccuracy may still be unavoidable due to the following reasons: 1) Due to the limited transmit power at the mobile station and the lack of beamforming gains for uplink pilot symbols, the accuracy of TDD-based CSI estimation through channel reciprocity is limited; 2) In mmWave M-MIMO systems (a large number of antennas can be easily packed into a small form factor due to the short wavelength), the channel coherence time is around an order of magnitude lower than that of microwave bands since Doppler shifts scale linearly with frequencies. This short channel coherence time implies that uplink CSI estimation is challenging. Therefore, it remains very relevant to investigate the impacts of imperfect CSI on M-MIMO cellular systems even in the TDD mode with channel reciprocity.

be viewed as a means to balance the trade-off between CSI accuracy and acquisition costs. The $B$-bit limited CSI for each user $n$ can be modeled based on a vector quantization codebook $\mathcal{B}_n \triangleq \{\mathbf{c}_n^1, \ldots, \mathbf{c}_n^{2^B}\}$, where $\mathbf{c}_n^i \in \mathbb{C}^M$, $i = 1, \ldots, 2^B$, denotes a codeword. With the CSI $\mathbf{h}_n[t]$ in time $t$, a codeword for each user $n$ is chosen by:

$$i_n^*[t] = \arg\max_{j\in\{1,\ldots,2^B\}} \left|\mathbf{h}_n^\dagger[t]\mathbf{c}_n^j\right| = \arg\min_{j\in\{1,\ldots,2^B\}} \sin^2(\angle(\mathbf{h}_n[t], \mathbf{c}_n^j)), \quad (3)$$

where $i_n^*[t]$ denotes the index of the chosen codeword. We let $\widehat{\mathbf{H}}[t] \in \mathbb{C}^{N\times M}$ denote the corresponding channel gain matrix in time-slot $t$ by aggregating all codewords $i_n^*[t]$, $\forall n$. Then, by treating $\widehat{\mathbf{H}}[t]$ as if it is the accurate CSI, the BS performs MF beamforming to construct $N$ spatial channels. However, due to the inaccuracy of $\widehat{\mathbf{H}}[t]$, multi-user interference may become non-negligible. Clearly, the impact of multi-user interference depends heavily on the codebook size $2^B$ and the design of the quantization codebook.

Let $\mathcal{C}_{\mathbf{H}[t]|\widehat{\mathbf{H}}[t]}$ denote the actual MF rate region achieved under $\mathbf{H}[t]$ based on the belief that $\widehat{\mathbf{H}}[t]$ is the accurate CSI. Also, let $\widehat{\mathbf{H}}_1[t]$ and $\widehat{\mathbf{H}}_2[t]$ represent two estimated CSI values obtained by using $B_1$ and $B_2$ bits, respectively. Further, we let $\mathcal{C}_{\mathbf{H}[t]}$ denote the original MF achievable rate region under full CSI $\mathbf{H}[t]$ . Then, one can show the following inclusion result of the MF achievable rate regions under limited CSI in M-MIMO networks (the proof is relegated to Appendix A):

**Lemma 1** (MF Rate Region Inclusion)**.** *If $B_1 \leq B_2$, then there exists a CSI quantization scheme under which $\mathcal{C}_{\mathbf{H}[t]|\widehat{\mathbf{H}}_1[t]} \subseteq \mathcal{C}_{\mathbf{H}[t]|\widehat{\mathbf{H}}_2[t]}$. Further, $\mathcal{C}_{\mathbf{H}[t]|\widehat{\mathbf{H}}[t]} \to \mathcal{C}_{\mathbf{H}[t]}$ as $B \to \infty$.*

**4) Queueing Model:** As illustrated in Fig. 1, the BS maintains a separate queue for each user. Let $a_n[t]$ denote the number of packets injected into queue $n$ in time-slot $t$. As shown in Fig. 1, the arrival processes $\{a_n[t]\}$, $\forall n$, are controlled by a congestion controller. Also, we assume that there exists a finite constant $A^{\max}$ such that $a_n[t] \leq A^{\max}$, $\forall n, t$. Let $\mathbf{s}_B[t] \triangleq [s_{B,1}[t], \ldots, s_{B,N}[t]]^\top$ denote the scheduled service rate vector in time-slot $t$ based on the belief that the current $B$-bit limited CSI is accurate (the scheduling algorithm that determines $\mathbf{s}_B[t]$ will be presented in Section III). Then, the queue-length of each user evolves as follows: $q_n[t+1] = \left(q_n[t] - s_{B,n}[t] + a_n[t]\right)^+$, $\forall n$, where $(\cdot)^+ \triangleq \max(0, \cdot)$. Let $\mathbf{q}[t] = [q_1[t]], \ldots, q_N[t]]^\top$. In this paper, we adopt the following notion of queue-stability (same as in [7], [8]): We say that a network is *stable* if the steady-state total queue-length is finite, i.e.,

$$\limsup_{t\to\infty} \mathbb{E}\left\{\|\mathbf{q}[t]\|_1\right\} < \infty. \quad (4)$$

**5) Problem Statement:** Let $\bar{a}_n \triangleq \lim_{T\to\infty} \frac{1}{T}\sum_{t=0}^{T-1} a_n[t]$ denote the average controlled arrival rate of user $n$. Each user $n$ is associated with a utility function $U_n(\bar{a}_n)$, which represents the utility gained by user $n$ when data is injected at rate $\bar{a}_n$. We assume that $U_n(\cdot)$, $\forall n$, is strictly concave, monotonically increasing, and twice continuously differentiable. We assume that $U_n(\cdot)$ satisfies the following strong concavity condition: there exist constants $0 < \phi < \Phi < \infty$ such that $\phi \leq -U_n''(a_n) \leq \Phi$, $\forall a_n \in [0, A^{\max}]$, where $A^{\max}$ is the maximum arrival rates for burst control. For example, $\log(a_n + \epsilon)$ is strongly concave for $\epsilon > 0$. Our goal is to maximize $\sum_{n=1}^N U_n(\bar{a}_n)$, subject to the MF beamforming rate region $\mathcal{C}_{\mathbf{H}[t]|\widehat{\mathbf{H}}[t]}$ due to limited CSI in each time-slot and the queue-stability constraint. Putting together the models presented above yields the following joint congestion control and scheduling (JCCS) optimization problem:

$$\textbf{JCCS: Maximize} \quad \sum_{n=1}^N U_n(\bar{a}_n)$$
$$\text{subject to} \quad \text{Queue-length stability constraint in (4)},$$
$$s_{B,n}[t] \in \mathcal{C}_{\mathbf{H}[t]|\widehat{\mathbf{H}}[t]},\ a_n[t] \in [0, A^{\max}]\ \forall n, t.$$

Note that, when perfect CSI is available ($B \to \infty$), the well-known QCS algorithmic framework [6]–[9] optimally solves Problem JCCR in the following sense: The $\bar{\mathbf{a}} \triangleq [\bar{a}_1, \ldots, \bar{a}_N]^\top$ obtained from the QCS algorithm achieves a utility optimality gap $O(1/K)$ at the expense of queue-length scaling as $O(K)$, where $K > 0$ is a system parameter. It will be clear in Section III-B that, from optimization theory perspective, this parameter $K$ can be interpreted as the inverse of the step-size in a stochastic subgradient descent method. Hence, the utility optimality gap can be made arbitrarily small by increasing $K$ asymptotically (implying an asymptotically large queueing delay). However, in M-MIMO cellular networks, it is not clear whether or not the QCS algorithmic framework will be optimal based on $B$-bit limited CSI. This constitutes the main discussions in the next section.

## III. Performance Analysis of the QCS Algorithm with Limited CSI

In this section, we first present a variant of the QCS algorithm adapted for M-MIMO with $B$-bit limited CSI in Section III-A. Then, we will examine a deterministic problem related to Problem JCCS in Section III-B to facilitate our discussions. The main theoretical results and their proofs will be presented in Sections III-C and III-D, respectively.

### A. The QCS Algorithm with Limited CSI

**Algorithm 1:** Queue-Length-Based Congestion Control and Scheduling for M-MIMO Cellular Networks with $B$-Bit CSI.

**Initialization:**

1. Select an appropriate $K > 0$ and an appropriate $B > 0$.

**Main Loop:**

2. *Queue-Length-Based MaxWeight Scheduler:* In time-slot $t \geq 1$, given the queue-length vector $\mathbf{q}[t] \triangleq [q_1[t], \ldots, q_N[t]]^\top$ and the $B$-bit estimated CSI $\widehat{\mathbf{H}}[t]$, the scheduler chooses a power allocation $\mathbf{p}[t] = [p_1[t], \ldots, p_N[t]]^\top$ such that the (believed) MF achievable rates $\mathbf{r}[t] = \arg\max_{\mathbf{x}\in\mathcal{C}_{\widehat{\mathbf{H}}[t]}} (\mathbf{q}[t])^\top \mathbf{x}$. As a result, the actual MF achievable service rates $s_{B,n}[t]$, $\forall n$, under $\mathbf{p}[t]$ are:

$$s_{B,n}[t] = \log_2\left(1 + \frac{p_n[t]\left|\mathbf{h}_n^\dagger[t]\widehat{\mathbf{h}}_n[t]\right|^2}{N_0 + \sum_{j=1,\neq n}^N p_j[t]\left|\mathbf{h}_n^\dagger[t]\widehat{\mathbf{h}}_j[t]\right|^2}\right). \quad (5)$$

3. *Congestion Controller:* Given the queue-length vector $\mathbf{q}[t] \triangleq [q_1[t], \ldots, q_N[t]]^\top$, the congestion controller chooses data inject rates $a_n[t]$, $\forall n$, which are integer-valued random variables satisfying:

$$\mathbb{E}\{a_n[t]|q_n[t]\} = \min\left\{U_n^{'-1}\left(\frac{q_n[t]}{K}\right), A^{\max}\right\}, \quad (6)$$

$$\mathbb{E}\{a_n^2[t]|q_n[t]\} \leq A_2^{\max} < \infty, \quad \forall q_n[t], \quad (7)$$

where $U_n^{'-1}(\cdot)$ represents the inverse function of first-order derivative of $U_n(\cdot)$. In (6) and (7), $A^{\max}$ and $A_2^{\max}$ are positive constants.

4. *Queue-Length Updates:* Update the queue-lengths as:

$$q_n[t+1] = (q_n[t] - s_{B,n}[t] + a_n[t])^+, \quad \forall n. \quad (8)$$

Let $t = t+1$. Go to Step 2 and repeat the scheduling and congestion control processes.

---

Some remarks on Algorithm 1 are in order: First, as mentioned in Sec. II, we focus on the case where $M \gg N$ in this paper so that the M-MIMO BS has sufficient spatial degrees of freedom to serve all users simultaneously. This would allow us to first simplify the problem and fully understand the effects of *imperfect CSI*. Once we gain a fundamental understanding on the impacts of imperfect CSI on M-MIMO cellular network optimization, we can extend these results to include user selection/grouping for the case with $M < N$ by imposing a constraint that only $N_0$ out of $N$ users are allowed to be served simultaneously and $N_0 \ll M$. Clearly, adding this discrete user selection scheduling constraint makes the MaxWeight scheduling subproblem in Step 2 in Algorithm 1 non-convex and NP-hard. Fortunately, there exists a large body of literature on user selection scheduling schemes (see, e.g., greedy maximal matching (see, e.g., [21]–[23] and references therein) for the QCS framework that have strong performance guarantees and can be applied in our problem setting. We note that a low-complexity scheduling scheme was recently proposed in [24], where the channel hardening effect in M-MIMO was exploited to yield a polynomial-time user selection algorithm. However, this user selection algorithm cannot be extended to our problem setting since our work differs [24] in the following aspects: i) Perfect CSI was assumed in [24] to enable the use of the channel hardening effect to approximate the rate calculation, while we do not assume perfect CSI in this paper. Because of this relaxation on perfect CSI assumption, the inter-user interference cannot be eliminated due to the CSI error, and hence it is unclear how well the channel hardening result would continue to hold. ii) The beamforming scheme used in [24] is the Linear Zero Forcing Beamforming (LZFBF), while we use the Matched-Filter (MF) Beamforming. As a result, the simplified approximate rate expression [24, Eq. (39)] does not apply in our problem setting.

Second, since user selection is not needed in our problem setting, now the main challenge is reflected in the limited and inaccurate CSI, which leads to suboptimal service rates in (5). This incurs service rate losses compared to the full CSI case, where the MaxWeight scheduler is of the form $\mathbf{s}[t] = \arg\max_{\mathbf{x}\in\mathcal{C}_{\mathbf{H}[t]}}(\mathbf{q}[t])^\top\mathbf{x}$. In what follows, we will focus on the impact of this inaccurate MaxWeight scheduling solution due to the $B$-bit limited CSI.

### *B. A Deterministic Problem*

To facilitate the presentation of our theoretical results in Section III-C, we first introduce a $K$-parameterized *deterministic* problem, where we assume that the channel state process is not random and fixed at its mean level. That is, the mean achievable rate region $\bar{\mathcal{C}}^B \triangleq \{\mathbf{r}|\mathbf{r} = \sum_{f=1}^F \pi_f \hat{\mathbf{r}}^{(f)}, \forall \mathbf{r}^{(f)} \in \mathcal{C}_{\mathbf{H}^{(f)}|\widehat{\mathbf{H}}_B^{(f)}}\}$, where $\mathcal{C}_{\mathbf{H}^{(f)}|\widehat{\mathbf{H}}_B^{(f)}}$ represents the actual MF rate region achieved under $\mathbf{H}^{(f)}$ based on the belief that the CSI is $\widehat{\mathbf{H}}_B^{(f)}$, i.e., the $B$-bit quantized CSI for state $f$. Also, the congestion control and scheduling variables are time-invariant, which are denoted as $a_n$ and $s_{B,n}$, $\forall n$, respectively. Then, the deterministic congestion control and scheduling problem ($K$-DJCCS) can be written as:

$$\begin{aligned} K\textbf{-DJCCS:}\ \text{Maximize} \quad & K\sum_{n=1}^N U_n(a_n) \\ \text{subject to} \quad & a_n - s_{B,n} \leq 0,\ \forall n, \\ & s_{B,n} \in \bar{\mathcal{C}}^B,\ a_n \in [0, a^{\max}],\ \forall n. \end{aligned}$$

Since Problem $K$-DJCCS is strictly convex, an optimal solution exists and is unique. Further, we associate dual variables $q_{B,n} \geq 0, \forall n$ with the constraints $a_n - s_{B,n} \leq 0, \forall n$, to obtain the Lagrangian as follows:

$$\Theta_K(\mathbf{q}_B) \triangleq \max_{\mathbf{a},\mathbf{s}_B\in\bar{\mathcal{C}}^B}\left\{K\sum_{n=1}^N U_n(a_n) + \sum_{n=1}^N q_{B,n}(s_{B,n} - a_n)\right\}, \quad (9)$$

where the vector $\mathbf{q}_B \triangleq [q_{B,1}, \ldots, q_{B,N}]^\top \in \mathbb{R}_+^N$ contains all dual variables. Then, the Lagrangian dual problem of Problem $K$-DJCCS can be written as:

$$\begin{aligned} K\textbf{-LD-JCCS:}\ \text{Minimize} \quad & \Theta_K(\mathbf{q}_B) \\ \text{subject to} \quad & \mathbf{q}_B \in \mathbb{R}_+^N. \end{aligned}$$

It can be verified that Problem $K$-DJCCS satisfies the Slater condition [25]. Hence, the optimal value of Problem $K$-LD-JCCS is equal to that of Problem $K$-DJCCS. Let $(\mathbf{a}_B^*, \mathbf{s}_B^*)$ and $\mathbf{q}_{B,(K)}^*$ be a pair of optimal primal and dual solutions. Then, $\mathbf{q}_{B,(K)}^*$ can be shown to have the following properties:

**Lemma 2** (Optimal dual solution scaling of the deterministic problem)**.** *For a given $K$, $\mathbf{q}_{B,(K)}^* = K\mathbf{q}_{B,(1)}^*$, or equivalently, $\mathbf{q}_{B,(K)}^*$ scales linearly as $O(K)$ and the slope is determined by the entries in $\mathbf{q}_{B,(1)}^*$. Further, $\mathbf{q}_{B_1,(1)}^* \geq \mathbf{q}_{B_2,(1)}^*$ if $B_1 \leq B_2$.*

Lemma 2 can be proved by examining the Karush-Kuhn-Tucker (KKT) conditions [25] of Problem $K$-DJCCS (see Appendix B). Also, by noting the fact that $K$ is just a scaling factor in the objective function and $\mathbf{a}_B^* = \mathbf{s}_B^*$ at optimality (by KKT conditions), we immediately have the following result for $\mathbf{a}_B^*$:

**Lemma 3** (Optimal primal solution of the deterministic problem)**.** *The optimal congestion control rate $\mathbf{a}_B^*$ is independent of $K$ and equal to the optimal service rate $\mathbf{s}_B^*$ over $\bar{\mathcal{C}}^B$.*

### C. Main Theoretical Results

In this section, we present the main performance analysis results of Algorithm 1. Our first result says that the steady-state queue-lengths $\mathbf{q}^{\infty}$ stay in a neighborhood of $\mathbf{q}^*_{B,(K)}$ (the existence of steady-state will also be proved later). Further, the scaling of the steady-state queue-length deviation from $\mathbf{q}^*_{B,(K)}$ exhibits a *phase-transition* phenomenon:

**Theorem 1** (Phase Transition Phenomenon of Queue-Length Scaling)**.** *For any $B$-bit CSI quantization scheme in Algorithm 1 with parameter $K$, there exists a critical value $B_{\rm cr}$ that is independent of $K$, such that the following hold:*

- *For all $0 < B < B_{\rm cr}$, $\mathbb{E}\{\|\mathbf{q}^{\infty} - \mathbf{q}^*_{B,(K)}\|\} = O(D_{(B)}K)$, where the parameter $D_{(B)} \geq 0$ depends on the quantization codebook design and shrinks as $B$ increases;*
- *For all $B \geq B_{\rm cr}$, $\mathbb{E}\{\|\mathbf{q}^{\infty} - \mathbf{q}^*_{B,(K)}\|\} = O(\sqrt{K})$.*

Collectively, Theorem 1 and Lemma 2 describe the steady-state queue-length behaviors. In particular, they show that if $B \geq B_{\rm cr}$, the steady state queue-length deviation is upper bounded by $O(\sqrt{K})$, which is small compared to the magnitude of $\mathbf{q}^*_{B,(K)}$, which grows linearly as $O(K)$ and the slope is affected by $B$: the larger the value of $B$, the more gradual the slope. Note that the scaling of the queue-length deviation for $B \geq B_{\rm cr}$ is the same as the classical result under full CSI [12]. This implies an interesting and surprising insight that full CSI is not necessary to induce certain desirable queueing behaviors in M-MIMO cellular networks.

Now, let $a^{\infty}_{B,n} \triangleq \mathbb{E}\{\min\{U_n^{'-1}(q^{\infty}_n/K), a^{\max}\}\}$, $\forall n$, be the steady-state congestion control rates under some $B$-bit CSI quantization and let $\mathbf{a}^{\infty}_B \triangleq [a^{\infty}_{B,1}, \ldots, a^{\infty}_{B,N}]^{\top}$. Our second main result is on the scaling of $\mathbf{a}^{\infty}_B$'s deviation from $\mathbf{a}^*_B$:

**Theorem 2** (Phase Transition Phenomenon of Congestion Control Rate Scaling)**.** *For any $B$-bit CSI quantization scheme in Algorithm 1 with parameter $K$, there exists a critical value $B_{\rm cr}$ (same as in Theorem 1) such that the following hold:*

- *For all $0 < B < B_{\rm cr}$, $\|\mathbf{a}^{\infty}_B - \mathbf{a}^*_B\| = O(D_{(B)})$, where the parameter $D_{(B)} \geq 0$ is the same as in Theorem 1;*
- *For all $B \geq B_{\rm cr}$, $\|\mathbf{a}^{\infty}_B - \mathbf{a}^*_B\| = O(1/\sqrt{K})$.*

Similar to the results in Theorem 1, Theorem 2 combined with Lemma 3 suggest that a phase transition phenomenon also exists in $\mathbf{a}^{\infty}_B$: When $B < B_{\rm cr}$, parameter $K$ becomes ineffective in the control of $\mathbf{a}^{\infty}_B$'s deviation from $\mathbf{a}^*_B$. On the other hand, when $B \geq B_{\rm cr}$, $\mathbf{a}^{\infty}_B$'s deviation from $\mathbf{a}^*_B$ scales as $O(1/\sqrt{K})$ and can be made arbitrarily small by increasing $K$. Since this $O(1/\sqrt{K})$ scaling is the same as that under full CSI [7], [8], $B_{\rm cr}$ represents the smallest codebook size of the given CSI quantization scheme that recovers the performance control functionality of parameter $K$.

### D. Proofs of the Main Theorems

In this subsection, we provide proofs for Theorems 1 and 2. To this end, we first show a positive Harris-recurrence result of the queue-length process, which implies the existence of steady-state and will be useful for proving Theorems 1 and 2 later. Let $\mathbb{1}_{\mathcal{A}}(\mathbf{x})$ be the indicator function that takes value 1 if $\mathbf{x} \in \mathcal{A}$ and 0 otherwise. The queue-length positive Harris-recurrence result can be stated as follows:

**Theorem 3** (Queue-Length Positive Recurrence)**.** *Consider a Lyapunov function $V(\mathbf{q}[t]) \triangleq \frac{1}{2K}\|\mathbf{q}[t] - \mathbf{q}^*_{B,(K)}\|^2$ for a given $K$. For the scheduler (5) and congestion controller (6)–(7), there exist constants $\delta, \eta > 0$, both independent of $K$, such that the queue-length process $\{\mathbf{q}[t]\}_{t=0}^{\infty}$ satisfies the following conditional mean drift condition:*

$$\begin{aligned}\mathbb{E}\{\Delta V(\mathbf{q}[t]|\mathbf{q}[t])\} &\triangleq \mathbb{E}\{V(\mathbf{q}[t+1]) - V(\mathbf{q}[t])|\mathbf{q}[t]\}\\ &\leq -\frac{\delta}{\Phi K}\big\|\mathbf{q}[t] - \mathbf{q}^*_{B,(K)}\big\|\mathbb{1}_{\mathcal{B}^c}(\mathbf{q}[t]) + \eta\mathbb{1}_{\mathcal{B}}(\mathbf{q}[t]), \quad (10)\end{aligned}$$

*where $\mathcal{B} \triangleq \{\mathbf{q} \in \mathbb{Z}^N_+ | \|\mathbf{q} - \mathbf{q}^*_{B,(K)}\| \leq \beta K\}$ for some constant $\beta > 0$ and $\mathcal{B}^c$ denotes the complement of $\mathcal{B}$ in $\mathbb{Z}^N_+$.*

We relegate the proof details of Theorem 3 to Appendix C. The inequality in (10) shows that the conditional mean drift is negative when the deviation of the queue-length vector $\mathbf{q}[t]$ away from $\mathbf{q}^*_{B,(K)}$ is sufficiently large. Since (10) is exactly the Foster-Lyapunove criterion [26, Proposition I.5.3], $\{\mathbf{q}[t]\}_{t=0}^{\infty}$ is positive recurrent, a steady-state distribution of queue-lengths exists. We denote the queue-length vector in steady-state as $\mathbf{q}^{\infty}$. With Theorem 3, we are now in a position to prove Theorem 1.

*Proof of Theorem 1.* To prove Theorem 1, we use an $\alpha$-parameterized quadratic Lyapunov function: $V_{\alpha}(\mathbf{q}[t]) = \frac{1}{2K^{\alpha}}\|\mathbf{q}[t] - \mathbf{q}^*_{B,(K)}\|^2$, where the parameter $\alpha \in \{0, 1\}$ and its value will be specified later. Different choices of the $\alpha$ value would lead to different Lyapunov functions, which subsequently lead to different scaling laws for different CSI accuracy levels. Following similar steps in the proof of Theorem 3 (see Appendix C), we can bound the conditional mean Lyapunov drift as follows:

$$\begin{aligned}&\mathbb{E}\{V_{\alpha}(\mathbf{q}[t+1]) - V_{\alpha}(\mathbf{q}[t])|\mathbf{q}[t]\}\\ &\overset{(a)}{\leq} \frac{1}{K^{\alpha}}(\mathbf{q}[t] - \mathbf{q}^*_{B,(K)})^{\top}(\mathbb{E}\{\mathbf{a}[t]|\mathbf{q}[t]\} - \mathbf{s}^*_B) +\\ &\quad \frac{1}{K^{\alpha}}\mathbb{E}\{(\mathbf{q}[t] - \mathbf{q}^*_{B,(K)})^{\top}(\mathbf{s}^*_B - \mathbf{s}_B[t])|\mathbf{q}[t]\} + \frac{D_0}{K^{\alpha}},\\ &\overset{(b)}{\leq} \frac{1}{K^{\alpha}}\Big[-\frac{1}{\Phi K}\big\|\mathbf{q}[t] - \mathbf{q}^*_{B,(K)}\big\|^2 + D_0\Big] +\\ &\quad \frac{1}{K^{\alpha}}\mathbb{E}\Big\{(\mathbf{q}[t] - \mathbf{q}^*_{B,(K)})^{\top}(\mathbf{s}^*_B - \mathbf{s}_B[t])\big|\mathbf{q}[t]\Big\}\\ &\overset{(c)}{\leq} \frac{1}{K^{\alpha}}\Big[-\frac{1}{\Phi K}\big\|\mathbf{q}[t] - \mathbf{q}^*_{B,(K)}\big\|^2 + D_0\Big] +\\ &\quad \frac{1}{K^{\alpha}}\mathbb{E}\Big\{(\mathbf{q}[t])^{\top}(\mathbf{s}^* - \mathbf{s}_B[t])\big|\mathbf{q}[t]\Big\}, \quad (11)\end{aligned}$$

where $D_0 \triangleq \frac{N}{2}(A_2^{\max} + (s^{\max})^2)$ and $\mathbf{s}^* \triangleq \lim_{B\to\infty}\mathbf{s}^*_B$. In (11), $(a)$ follows from adding and subtracting $\mathbf{s}^*_B$; $(b)$ follows from (36); and $(c)$ follows from $\mathbf{s}^*_B \leq \mathbf{s}^*$ (by Lemma 1) and the scheduler design, which implies $(\mathbf{q}^*_{B,(K)})^{\top}\mathbf{s}_B[t] \leq (\mathbf{q}^*_{B,(K)})^{\top}\mathbf{s}^*_B$. Next, consider the $T$-step conditional mean Lyapunov drift. For any $\mathbf{q}[0] \geq \mathbf{0}$, we have that

$$\begin{aligned}\mathbb{E}\{V_{\alpha}(\mathbf{q}[T])|\mathbf{q}[0]\} - V_{\alpha}(\mathbf{q}[0]) &= \sum_{t=0}^{T-1}\mathbb{E}\{V(\mathbf{q}[t+1]) - V(\mathbf{q}[t])|\mathbf{q}[0]\}\\ &\overset{(a)}{=} \sum_{t=0}^{T-1}\sum_{\mathbf{q}\in\mathcal{Z}^N_+}\big[\Pr(\mathbf{q}[t] = \mathbf{q}|\mathbf{q}[0])\mathbb{E}\big\{V_{\alpha}(\mathbf{q}[t+1]) - V_{\alpha}(\mathbf{q}[t])|\mathbf{q}[t] = \mathbf{q}\big\}\big]\end{aligned}$$

$$\overset{(b)}{\leq}\sum_{t=0}^{T-1}\sum_{\mathbf{q}\in\mathcal{Z}_+^N}\Pr(\mathbf{q}[t]=\mathbf{q}|\mathbf{q}[0])\Big\{\frac{1}{K^\alpha}\Big[\frac{-1}{\Phi K}\big\|\mathbf{q}[t]-\mathbf{q}^*_{B,(K)}\big\|^2+D_0\Big]\Big\}$$
$$+\sum_{t=0}^{T-1}\sum_{\mathbf{q}\in\mathcal{Z}_+^N}\Pr(\mathbf{q}[t]=\mathbf{q}|\mathbf{q}[0])\Big\{\frac{1}{K^\alpha}\mathbb{E}\Big\{\mathbf{q}^\top(\mathbf{s}^*-\mathbf{s}_B[t])\Big\}\Big\}, \quad (12)$$

where $(a)$ follows from the fact that $\mathbf{q}[t]$ is a discrete state Markov chain in $\mathbb{Z}_+^N$ and $(b)$ follows from (11). Note that for any $\mathbf{q}[t]\in\mathbb{Z}_+^N$, $\lim_{T\to\infty}\frac{1}{T}\sum_{t=0}^{T-1}\Pr(\mathbf{q}[t]=\mathbf{q}|\mathbf{q}[0])=\pi_{\mathbf{q}}^\infty$, where $\pi_{\mathbf{q}}^\infty$ denotes the stationary distribution of the Markov chain $\mathbf{q}[t]$. Moving $V(\mathbf{q}[0])$ to the right hand side, dividing both sides by $T$, and letting $T\to\infty$ yields:

$$0\leq J+\sum_{\mathbf{q}\in\mathbb{Z}_+^N}\pi_{\mathbf{q}}^\infty(\mathbf{q})^\top(\mathbf{s}^*-\mathbf{s}_B^\infty)=J+\mathbb{E}\big\{(\mathbf{q}^\infty)^\top(\mathbf{s}^*-\mathbf{s}_B^\infty\big\}, \quad (13)$$

where $J\triangleq\lim_{T\to\infty}\frac{1}{T}\sum_{t=0}^{T-1}\sum_{\mathbf{q}\in\mathcal{Z}_+^N}\Pr(\mathbf{q}[t]=\mathbf{q}|\mathbf{q}[0])\{\frac{1}{K^\alpha}[\frac{-1}{\Phi K}\|\mathbf{q}[t]-\mathbf{q}^*_{(K)}\|^2+D_0]\}$, $\mathbf{s}_B^\infty\triangleq\arg\max_{\mathbf{x}\in\mathcal{C}_{\mathbf{H}[\infty]|\widehat{\mathbf{H}}[\infty]}}(\mathbf{q}^\infty)^\top\mathbf{x}$ represents the steady-state service rates with $B$-bit CSI.

Next, consider the term $\mathbb{E}\big\{(\mathbf{q}^\infty)^\top(\mathbf{s}^*-\mathbf{s}_B^\infty)\big\}$ in (13). For any given realization of $\mathbf{q}^\infty$ in the steady-state, from the design of the MaxWeight scheduler in (5), we have that

$$(\mathbf{q}^\infty)^\top\mathbf{s}^*\leq\max_{\mathbf{x}\in\mathcal{C}_{\mathbf{H}[\infty]}}(\mathbf{q}^\infty)^\top\mathbf{x}=(\mathbf{q}^\infty)^\top\mathbf{s}^\infty. \quad (14)$$

where $\mathbf{s}^\infty\triangleq\lim_{B\to\infty}\mathbf{s}_B^\infty$ and $\mathbf{H}[\infty]$ represent the full CSI in the steady state. Hence, for any realization of $\mathbf{q}^\infty$ such that $\mathbf{q}^\infty\neq\rho\mathbf{s}^*$ for some $\rho\in\mathbb{R}$, if $B$ is sufficiently large, we must have $(\mathbf{q}^\infty)^\top\mathbf{s}^*-(\mathbf{q}^\infty)^\top\mathbf{s}_B^\infty\leq 0$. Hence, there exists a critical value $B_{\rm cr}$ such that for all $B>B_{\rm cr}$, the average value of $(\mathbf{q}^\infty)^\top\mathbf{s}^*-(\mathbf{q}^\infty)^\top\mathbf{s}_B^\infty$ can be made non-positive, i.e., $\mathbb{E}\big\{(\mathbf{q}^\infty)^\top(\mathbf{s}^*-\mathbf{s}_B^\infty)\big\}\leq 0$. Hence, we consider two cases based on the positivity of $\mathbb{E}\big\{(\mathbf{q}^\infty)^\top(\mathbf{s}^*-\mathbf{s}_B^\infty)\big\}$ as follows:

*Case I):* $B\geq B_{\rm cr}$ such that $\mathbb{E}\big\{(\mathbf{q}^\infty)^\top(\mathbf{s}^*-\mathbf{s}_B^\infty)\big\}\leq 0$: In this case, it follows from (13) that

$$0\leq\lim_{T\to\infty}\frac{1}{T}\sum\nolimits_{t=0}^{T-1}\sum\nolimits_{\mathbf{q}\in\mathcal{Z}_+^N}\Pr(\mathbf{q}[t]=\mathbf{q}|\mathbf{q}[0])\times$$
$$\Big\{\frac{1}{K^\alpha}\Big[-\frac{1}{\Phi K}\big\|\mathbf{q}[t]-\mathbf{q}^*_{B,(K)}\big\|^2+D_0\Big]\Big\}. \quad (15)$$

We now consider the term in the second line in (15) by setting $\alpha=0$. Similar to the proof of Theorem 3, suppose that $\big\|\mathbf{q}[t]-\mathbf{q}^*_{B,(K)}\big\|\geq\beta\sqrt{K}$, where $\beta$ will be specified shortly. This implies that $\frac{1}{\|\mathbf{q}[t]-\mathbf{q}^*_{B,(K)}\|}\leq\frac{1}{\beta}$. Then, the second line in (15) can be upper bounded as:

$$-\frac{1}{\Phi K}\big\|\mathbf{q}[t]-\mathbf{q}^*_{B,(K)}\big\|^2+D_0=-\frac{1}{\Phi\sqrt{K}}\big\|\mathbf{q}[t]-\mathbf{q}^*_{B,(K)}\big\|\times$$
$$\left(\frac{\|\mathbf{q}[t]-\mathbf{q}^*_{B,(K)}\|}{\sqrt{K}}+\frac{D_0\Phi\sqrt{K}}{\|\mathbf{q}[t]-\mathbf{q}^*_{B,(K)}\|}\right)$$
$$\leq-\frac{1}{\Phi\sqrt{K}}\big\|\mathbf{q}[t]-\mathbf{q}^*_{B,(K)}\big\|\left(\beta-\frac{D_0\Phi}{\beta}\right). \quad (16)$$

Hence, by choosing $\beta>\sqrt{D_0\Phi}$, we have

$$-\frac{1}{\Phi K}\big\|\mathbf{q}[t]-\mathbf{q}^*_{B,(K)}\big\|^2+D_0\leq-\frac{\hat{\delta}}{\Phi\sqrt{K}}\big\|\mathbf{q}[t]-\mathbf{q}^*_{B,(K)}\big\|, \quad (17)$$

where $\hat{\delta}=\beta-\frac{D_0\Phi}{\beta}>0$. Plugging in $\beta>\sqrt{D_0\Phi}$ to define a ball $\mathcal{B}\triangleq\{\mathbf{q}:\|\mathbf{q}-\mathbf{q}^*_{B,(K)}\|\leq\sqrt{D_0\Phi K}\}$, we have that if $\mathbf{q}[t]\in\mathcal{B}^c$, the following holds:

$$-\frac{1}{\Phi K}\big\|\mathbf{q}[t]-\mathbf{q}^*_{B,(K)}\big\|^2+D_0\leq-\frac{\delta}{\sqrt{K}}\|\mathbf{q}[t]-\mathbf{q}^*_{B,(K)}\|.$$

On the other hand, when $\|\mathbf{q}[t]-\mathbf{q}^*_{B,(K)}\|\leq\sqrt{D_0\Phi K}$, it is clear that $-(1/\Phi K)\big\|\mathbf{q}[t]-\mathbf{q}^*_{B,(K)}\big\|^2+D_0\leq\eta$ for some $\eta>0$. Combining these facts, we have

$$-\frac{1}{\Phi K}\big\|\mathbf{q}[t]-\mathbf{q}^*_{B,(K)}\big\|^2+D_0$$
$$\leq-\frac{\delta}{K}\|\mathbf{q}[t]-\mathbf{q}^*_{B,(K)}\|\mathbb{1}_{\mathcal{B}^c}(\mathbf{q}[t])+\eta\mathbb{1}_{\mathcal{B}}(\mathbf{q}[t]). \quad (18)$$

Substituting (18) into (15) yields:

$$0\leq\lim_{T\to\infty}\frac{1}{T}\sum_{t=0}^{T-1}\sum_{\mathbf{q}\in\mathcal{Z}_+^N}\Pr(\mathbf{q}[t]=\mathbf{q}|\mathbf{q}[0])\times$$
$$\Big(-\frac{\delta}{K}\|\mathbf{q}[t]-\mathbf{q}^*_{B,(K)}\|\mathbb{1}_{\mathcal{B}^c}(\mathbf{q})+\eta\mathbb{1}_{\mathcal{B}}(\mathbf{q})\Big)$$
$$=\eta\sum_{\mathbf{q}\in\mathcal{B}}\pi_{\mathbf{q}}^\infty-\frac{\delta}{\sqrt{K}}\sum_{\mathbf{q}\in\mathcal{B}^c}\|\mathbf{q}-\mathbf{q}^*_{B,(K)}\|\pi_{\mathbf{q}}^\infty. \quad (19)$$

where we use the fact that, $\forall\mathbf{q}\in\mathcal{Z}_+^N$, $\lim_{T\to\infty}\frac{1}{T}\sum_{t=0}^{T-1}\Pr\{\mathbf{q}[t]=\mathbf{q}|\mathbf{q}[0]\}=\pi_{\mathbf{q}}^\infty$. Re-arranging the terms and with some manipulations, the above inequality can be written as:

$$\frac{\delta}{\sqrt{K}}\sum_{\mathbf{q}\in\mathcal{Z}_+^N}\|\mathbf{q}-\mathbf{q}^*_{B,(K)}\|\pi_{\mathbf{q}}^\infty\leq\sum_{\mathbf{q}\in\mathcal{B}}\left(\eta+\frac{\delta}{\sqrt{K}}\|\mathbf{q}-\mathbf{q}^*_{B,(K)}\|\right)\pi_{\mathbf{q}}^\infty$$
$$\leq(\eta+\delta\beta)\sum_{\mathbf{q}\in\mathcal{B}}\pi_{\mathbf{q}}^\infty\leq(\eta+\delta\beta), \quad (20)$$

where the second inequality follows from the definition of $\mathcal{B}$. Note here that the left-hand-side is precisely $\frac{\delta}{\sqrt{K}}\mathbb{E}\{\|\mathbf{q}^\infty-\mathbf{q}^*_{B,(K)}\|\}$. Thus, multiplying both sides by $\sqrt{K}/\delta$, we have:

$$\mathbb{E}\{\|\mathbf{q}^\infty-\mathbf{q}^*_{B,(K)}\|\}\leq\left(\beta+\frac{\eta}{\delta}\right)\sqrt{K}=O(\sqrt{K}). \quad (21)$$

*Case II):* $B\leq B_{\rm cr}$ such that $\mathbb{E}\big\{(\mathbf{q}^\infty)^\top(\mathbf{s}^*-\mathbf{s}_B^\infty)\big\}>0$: In this case, we set $\alpha=1$. It thus follows from (11) that:

$$\mathbb{E}\big\{\Delta V_1(\mathbf{q}[t])|\mathbf{q}[t]\big\}\leq-\frac{1}{\Phi K^2}\left\|\mathbf{q}[t]-\mathbf{q}^*_{B,(K)}\right\|^2+$$
$$\frac{1}{K}\|\mathbf{q}[t]-\mathbf{q}^*_{B,(K)})^\top\|D_{(B)}+\frac{D_0}{K}, \quad (22)$$

where $D_{(B)}$ is defined in the proof of Theorem 3 (cf. Eq. (33)). Note that (22) is identical to (37). Then, following exactly the same steps as in the proof of Theorem 3, we have:

$$\mathbb{E}\{\Delta V_1(\mathbf{q}[t])|\mathbf{q}[t]=\mathbf{q}\}\leq-\frac{\delta_1}{K}\|\mathbf{q}-\mathbf{q}^*_{B,(K)}\|\mathbb{1}_{\mathcal{B}_1^c}(\mathbf{q})+\eta_1\mathbb{1}_{\mathcal{B}_1}(\mathbf{q}).$$

where $\delta_1$, $\eta_1$, and $\mathcal{B}_1$ are the same as in the proof of Theorem 3. Then, it follows from (12) that

$$\mathbb{E}\{V_1(\mathbf{q}[T]|\mathbf{q}[0])\}-V_1(\mathbf{q}[0])\leq\eta_1\sum_{\mathbf{q}\in\mathcal{B}_1}\sum_{t=0}^{T-1}\Pr\{\mathbf{q}[t]=\mathbf{q}|\mathbf{q}[0]\}$$
$$-\frac{\delta_1}{K}\sum_{\mathbf{q}\in\mathcal{B}_1^c}\|\mathbf{q}-\mathbf{q}^*_{(K)}\|\sum_{t=0}^{T-1}\Pr\{\mathbf{q}[t]=\mathbf{q}|\mathbf{q}[0]\}. \quad (23)$$

Following similar steps as in Case I to divide $T$ on both sides on (23) and let $T \to \infty$, we have $0 \leq \eta_1 \sum_{\mathbf{q}\in\mathcal{B}_1} \pi_{\mathbf{q}}^{\infty} - \frac{\delta_1}{K} \sum_{\mathbf{q}\in\mathcal{B}_1^c} \|\mathbf{q} - \mathbf{q}_{B,(K)}^*\| \pi_{\mathbf{q}}^{\infty}$. Re-arranging the terms and with some manipulations, the above inequality can be written as:

$$\begin{aligned}
&\frac{\delta_1}{K} \sum_{\mathbf{q}\in\mathcal{Z}_+^N} \|\mathbf{q} - \mathbf{q}_{B,(K)}^*\| \pi_{\mathbf{q}}^{\infty} \\
&\leq \sum_{\mathbf{q}\in\mathcal{B}_1} \left(\eta_1 + \frac{\delta_1}{K}\|\mathbf{q} - \mathbf{q}_{B,(K)}^*\|\right) \pi_{\mathbf{q}}^{\infty} \\
&\leq (\eta_1 + \delta_1\beta_1) \sum_{\mathbf{q}\in\mathcal{B}} \pi_{\mathbf{q}}^{\infty} \leq (\eta_1 + \delta_1\beta_1),
\end{aligned}$$

where $\beta_1$ is the same as in the proof of Theorem 3. Note that the left-hand-side is $\frac{\delta_1}{K}\mathbb{E}\{\|\mathbf{q}^{\infty} - \mathbf{q}_{B,(K)}^*\|\}$. Multiplying both sides by $\frac{K}{\delta_1}$, we have:

$$\begin{aligned}
&\mathbb{E}\{\|\mathbf{q}^{\infty} - \mathbf{q}_{B,(K)}^*\|\} \leq \left(\beta_1 + \frac{\eta_1}{\delta_1}\right) K \\
&= \left(\left[(D_{(B)}\Phi) + \sqrt{(D_{(B)}\Phi)^2 + 4D_0\Phi}\right] + \frac{\eta}{\delta}\right) K \\
&= O(D_{(B)}K).
\end{aligned}$$

This completes the proof of Theorem 1. □

One important remark regarding $B_{\rm cr}$ is in order: From the proof of Theorem 1, we can see that $B_{\rm cr}$ is determined by the condition $\mathbb{E}\{(\mathbf{q}^{\infty})^{\top}(\mathbf{s}^* - \mathbf{s}_B^{\infty})\} = 0$. Note that

$$\begin{aligned}
&\mathbb{E}\{(\mathbf{q}^{\infty})^{\top}(\mathbf{s}^* - \mathbf{s}_B^{\infty})\} = \mathbb{E}\{(\mathbf{q}^{\infty})^{\top}(\mathbf{s}^* - \mathbf{s}^{\infty} + \mathbf{s}^{\infty} - \mathbf{s}_B^{\infty})\} \\
&= \underbrace{\mathbb{E}\{(\mathbf{q}^{\infty})^{\top}(\mathbf{s}^* - \mathbf{s}^{\infty})\}}_{<0} + \underbrace{\mathbb{E}\{(\mathbf{q}^{\infty})^{\top}(\mathbf{s}^{\infty} - \mathbf{s}_B^{\infty})\}}_{\downarrow 0 \text{ as } B\to 0}
\end{aligned}$$

From the analysis in the proof of Theorem 1, we know that $\mathbb{E}\{(\mathbf{q}^{\infty})^{\top}(\mathbf{s}^* - \mathbf{s}^{\infty})\} < 0$ and $\mathbb{E}\{(\mathbf{q}^{\infty})^{\top}(\mathbf{s}^{\infty} - \mathbf{s}_B^{\infty})\} \downarrow 0$ as $B \to \infty$, both of which are due to the MaxWeight scheduling property. Therefore, $B_{\rm cr}$ depends on the quantities $\mathbf{q}^{\infty}$, $\mathbf{s}^*$, and $\mathbf{s}^{\infty}$, which determine how negative the term $\mathbb{E}\{(\mathbf{q}^{\infty})^{\top}(\mathbf{s}^* - \mathbf{s}^{\infty})\}$ is. Note that the quantities $\mathbf{q}^{\infty}$, $\mathbf{s}^*$, and $\mathbf{s}^{\infty}$ are determined by the specific problem instance factors, such as the utility functions $U_n(\cdot)$, $\forall n$, the mean MF achievable rate region $\bar{\mathcal{C}}$, etc.

*Proof of Theorem 2.* To show the results in Theorem 2, we first note that $\mathbb{E}\{a_n[t]|q_n[t]\} = \min\{U_n'^{-1}(\frac{q_n[t]}{K}, A^{\max})\}$ and $a_n^* = U_n'^{-1}(\frac{q_n^*}{K})$, $\forall n$. Thus, we have:

$$\begin{aligned}
&\|\mathbf{a}_B^{\infty} - \mathbf{a}_B^*\| \leq \|\mathbf{a}_B^{\infty} - \mathbf{a}_B^*\|_1 \\
&= \sum_{n=1}^{N} \left|\mathbb{E}\Big\{\min\Big\{U_n'^{-1}\Big(\frac{q_n^{\infty}}{K}, A^{\max}\Big)\Big\}\Big\} - U_n'^{-1}\Big(\frac{q_{B,(K),n}^*}{K}\Big)\right| \\
&\overset{(a)}{\leq} \sum_{n=1}^{N} \mathbb{E}\left\{\left|\min\Big\{U_n'^{-1}\Big(\frac{q_n^{\infty}}{K}, A^{\max}\Big)\Big\} - U_n'^{-1}\Big(\frac{q_{B,(K),n}^*}{K}\Big)\right|\right\} \\
&\overset{(b)}{\leq} \sum_{n=1}^{N} \mathbb{E}\left\{\left|U_n'^{-1}\Big(\frac{q_n^{\infty}}{K}\Big) - U_n'^{-1}\Big(\frac{q_{B,(K),n}^*}{K}\Big)\right|\right\} \\
&\overset{(c)}{=} \sum_{n=1}^{N} \mathbb{E}\left\{\left|\Big[U_n'^{-1}\Big(\frac{\tilde{q}_n}{K}\Big)\Big]'\Big(\frac{q_n^{\infty}}{K} - \frac{q_{B,(K),n}^*}{K}\Big)\right|\right\} \\
&\overset{(d)}{\leq} \sum_{n=1}^{N} \mathbb{E}\left\{\Big|\frac{1}{U_n''(\frac{\tilde{q}_n}{K})}\Big|\Big|\frac{q_n^{\infty}}{K} - \frac{q_{B,(K),n}^*}{K}\Big|\right\} \\
&\leq \sum_{n=1}^{N} \mathbb{E}\left\{\frac{1}{\phi K}\big|q_n^{\infty} - q_{B,(K),n}^*\big|\right\} = \frac{1}{\phi K}\mathbb{E}\big\{\big\|\mathbf{q}^{\infty} - \mathbf{q}_{B,(K)}^*\big\|_1\big\} \\
&\leq \frac{\sqrt{N}}{\phi K}\mathbb{E}\big\{\big\|\mathbf{q}^{\infty} - \mathbf{q}_{B,(K)}^*\big\|\big\}, \qquad (24)
\end{aligned}$$

where $(a)$ follows from Jensen's inequality and the convexity of the $L^1$-norm; $(b)$ follows from relaxing the projection onto $[0, A^{\max}]$; $(c)$ follows from the mean value theorem; and $(d)$ follows from the inverse function lemma. Recall in the proof of Theorem 1 (cf. (13)), we have $0 \leq J + \sum_{\mathbf{q}\in\mathbb{Z}_+^N} \pi_{\mathbf{q}}^{\infty} (\mathbf{q})^{\top}(\mathbf{s}^* - \mathbf{s}_B^{\infty}) = J + \mathbb{E}\big\{(\mathbf{q}^{\infty})^{\top}(\mathbf{s}^* - \mathbf{s}_B^{\infty})\big\}$. Again, based on the positivity of the term $\mathbb{E}\big\{(\mathbf{q}^{\infty})^{\top}(\mathbf{s}^* - \mathbf{s}_B^{\infty})\big\}$, we consider two cases:

*Case I):* $B > B_{\rm cr}$ such that $\mathbb{E}\big\{(\mathbf{q}^{\infty})^{\top}(\mathbf{s}^* - \mathbf{s}_B^{\infty})\big\} \leq 0$: In this case, we can again discard $\mathbb{E}\big\{(\mathbf{q}^{\infty})^{\top}(\mathbf{s}^* - \mathbf{s}_B^{\infty})\big\}$ in (13) and let $\alpha = 0$ to obtain:

$$\begin{aligned}
0 \leq \lim_{T\to\infty} \frac{1}{T} \sum\nolimits_{t=0}^{T-1} \sum\nolimits_{\mathbf{q}\in\mathcal{Z}_+^N} &\Pr(\mathbf{q}[t] = \mathbf{q}|\mathbf{q}[0]) \times \\
&\Big\{ - \frac{1}{\Phi K}\big\|\mathbf{q}[t] - \mathbf{q}_{B,(K)}^*\big\|^2\Big\} + D_0.
\end{aligned}$$

By re-arranging, multiplying both sides by $\Phi K$, and noting that $\lim_{T\to\infty} \frac{1}{T} \sum_{t=0}^{T-1} \Pr\{\mathbf{q}[t] = \mathbf{q}|\mathbf{q}[0]\} = \pi_{\mathbf{q}}^{\infty}$, we have

$$\mathbb{E}\big\{\|\mathbf{q}^{\infty} - \mathbf{q}_{B,(K)}^*\|^2\big\} \leq D_0\Phi K. \qquad (25)$$

It then follows from (24) that

$$\begin{aligned}
\|\mathbf{a}_B^{\infty} - \mathbf{a}_B^*\|^2 &\leq \left(\frac{\sqrt{N}}{\phi K}\mathbb{E}\big\{\big\|\mathbf{q}^{\infty} - \mathbf{q}_{B,(K)}^*\big\|\big\}\right)^2 \\
&\overset{(a)}{\leq} \frac{N}{\phi^2 K^2}\mathbb{E}\big\{\big\|\mathbf{q}^{\infty} - \mathbf{q}_{B,(K)}^*\big\|^2\big\} \overset{(b)}{\leq} \frac{N}{\phi^2 K^2} D_0\Phi K = \frac{N D_0}{\phi^2 K}, \qquad (26)
\end{aligned}$$

where $(a)$ follows from Jensen's inequality; and $(b)$ follows from (25). Taking square root on both sides of (26) yields $\|\mathbf{a}_B^{\infty} - \mathbf{a}_B^*\| = O(1/\sqrt{K})$.

*Case II):* $B \leq B_{\rm cr}$ such that $\mathbb{E}\big\{(\mathbf{q}^{\infty})^{\top}(\mathbf{s}^* - \mathbf{s}_B^{\infty})\big\} > 0$: In this case, we set $\alpha = 1$ and it follows from (11) that:

$$\begin{aligned}
\mathbb{E}\big\{\Delta V_1(\mathbf{q}[t])|\mathbf{q}[t]\big\} &\leq -\frac{1}{\Phi K^2}\Big\|\mathbf{q}[t] - \mathbf{q}_{B,(K)}^*\Big\|^2 + \\
&\qquad \frac{D_{(B)}}{K}\|\mathbf{q}[t] - \mathbf{q}_{B,(K)}^*)^{\top}\| + \frac{D_0}{K} \\
&= -\frac{1}{\Phi K^2}\left(\big\|\mathbf{q}[t] - \mathbf{q}_{B,(K)}^*\big\| - \frac{D_{(B)}\Phi K}{2}\right)^2 + D, \qquad (27)
\end{aligned}$$

where $D_{(B)}$ is defined in the proof of Theorem 3 (cf. Eq. (33)) and $D \triangleq \frac{D_{(B)}}{4} + \frac{D_0}{\Phi K}$. Telescoping the inequality in (27) from $t = 0$ to $T - 1$ yields:

$$\begin{aligned}
\mathbb{E}\{V_1(\mathbf{q}[T]|\mathbf{q}[0])\} - V_1(\mathbf{q}[0]) \leq &-\frac{1}{\Phi K^2}\sum_{t=0}^{T-1}\sum_{\mathbf{q}\in\mathbb{Z}_+^N} \Pr\{\mathbf{q}[t] = \mathbf{q}|\mathbf{q}[0]\} \\
&\times \left(\big\|\mathbf{q}[t] - \mathbf{q}_{B,(K)}^*\big\| - \frac{D_{(B)}\Phi K}{2}\right)^2 + DT. \qquad (28)
\end{aligned}$$

Dividing both sides of (28) by $\frac{T}{K^2}$, letting $T \to \infty$, and noting that $\lim_{T\to\infty} \frac{1}{T} \sum_{t=0}^{T-1} \Pr\{\mathbf{q}[t] = \mathbf{q}|\mathbf{q}[0]\} = \pi_{\mathbf{q}}^{\infty}$, $\forall \mathbf{q} \in \mathcal{Z}_+^N$, we have that:

$$\mathbb{E}\left\{\left(\left\|\mathbf{q}^{\infty}-\mathbf{q}^{*}_{B,(K)}\right\|-\frac{D_{(B)}\Phi K}{2}\right)^{2}\right\}\leq D\Phi K^{2}.$$

Taking square root on both sides yields:

$$\left[\mathbb{E}\left\{\left(\left\|\mathbf{q}^{\infty}-\mathbf{q}^{*}_{B,(K)}\right\|-\frac{D_{(B)}\Phi K}{2}\right)^{2}\right\}\right]^{\frac{1}{2}}\leq K\sqrt{D\Phi}. \tag{29}$$

Moreover, examining the left-hand-side of (29), we have

$$\begin{aligned}&\left[\mathbb{E}\left\{\left(\left\|\mathbf{q}^{\infty}-\mathbf{q}^{*}_{B,(K)}\right\|-\frac{D_{(B)}\Phi K}{2}\right)^{2}\right\}\right]^{\frac{1}{2}}\\&\overset{(a)}{\geq}\mathbb{E}\left\{\left[\left(\left\|\mathbf{q}^{\infty}-\mathbf{q}^{*}_{B,(K)}\right\|-\frac{D_{(B)}\Phi K}{2}\right)^{2}\right]^{\frac{1}{2}}\right\}\\&=\mathbb{E}\left\{\left|\left\|\mathbf{q}^{\infty}-\mathbf{q}^{*}_{B,(K)}\right\|-\frac{D_{(B)}\Phi K}{2}\right|\right\}\\&\geq\mathbb{E}\left\{\left\|\mathbf{q}^{\infty}-\mathbf{q}^{*}_{B,(K)}\right\|-\frac{D_{(B)}\Phi K}{2}\right\}\\&=\mathbb{E}\{\left\|\mathbf{q}^{\infty}-\mathbf{q}^{*}_{B,(K)}\right\|\}-\frac{D_{(B)}\Phi K}{2},\end{aligned} \tag{30}$$

where $(a)$ follows from Jensen's inequality. Combining (24), (29), and (30) yields:

$$\begin{aligned}\left\|\mathbf{a}^{\infty}_{B}-\mathbf{a}^{*}_{B}\right\|&\leq\frac{\sqrt{N}}{\phi K}\mathbb{E}\{\left\|\mathbf{q}^{\infty}-\mathbf{q}^{*}_{B,(K)}\right\|\}\\&=\frac{\sqrt{N}}{\phi K}\left(\frac{D_{(B)}\Phi K}{2}+K\sqrt{D\Phi}\right)=O(D_{(B)}).\end{aligned}$$

Note that Cases I and II are exactly the same results as stated in Theorem 2. This completes the proof. □

## IV. Numerical Results

In this section, we conduct numerical experiments to verify the theoretical results presented in Section III. In our simulations, we use a 128-antenna M-MIMO base station with MF precoding to serve four users. Each user's channel is i.i.d. Rayleigh faded. The maximum total signal-to-noise ratio (SNR) of the BS is set to 30dB. We use $\log(\cdot+0.001)$ as the utility function for each user, i.e., the proportional fairness metric [10]. In our numerical studies, the channel states (i.e., the channel gain matrix $\mathbf{H}[t]$ in each time-slot $t$) are randomly generated in MATLAB. In the perfect CSI case, we directly use $\mathbf{H}[t]$ in each time slot $t$ as CSI input in Step 2 in Algorithm 1. We adopt the random vector quantization (RVQ) scheme, which has been widely used in the MIMO limited CSI feedback literature [14], [15], [18]. The value of $B$ is set to be 1, 2, 4, 8, 16, 32, 53, and 64, covering cases from the simplest two-state channel quantization to channel quantizations with high granularity.

We first study the impacts of $B$ on the delay performance. The results of average queue-length deviations with respect to the changes of $B$ are illustrated in Fig. 2. In Fig. 2, each solid curve represents the average queue-length deviation scaling with respect to $K$ under a certain CSI accuracy parameterized by $B$. For each scaling curve, we also plot an accompanying line (the red dash lines). The bottom 4 accompanying lines represent (starting from bottom) $0.44\sqrt{K}$, $0.5\sqrt{K}$, $0.58\sqrt{K}$, $0.58\sqrt{K}$, and $0.64\sqrt{K}$. They correspond to $B=64,53,32,16$, and 16, respectively. Fig. 2 shows that the average queue-length deviation curves sit below each accompanying line when $B\geq 16$, confirming that the average queue-length deviations are bounded by the $O(\sqrt{K})$ scaling. On the other hand, when $B<16$, there is no $O(\sqrt{K})$ accompanying lines that can dominate the average queue-length deviation curves, which means that the average queue-length deviation grows faster than the square root law and approximately exhibits a linear growth with respect to $K$. To see this, in Fig. 2, we plot 3 straight accompanying lines. We can see that the average queue-length deviation curves hovering around these linear scaling accompanying lines, confirming the linear scaling growth. Finally, combining two parts, we can see that $B=16$ is the critical point, where the phase transition from $O(K)$ scaling to $O(\sqrt{K})$ happens.

Also, when $B=64$, we can see that the queue-length deviations almost coincide with that in the full CSI case, showing that the 64-bit RVQ scheme is almost as accurate as full CSI. Note that, as discussed earlier, obtaining full CSI is costly or even unrealistic in practice: On one hand, if CSI is measured at the mobile station, then the mobile station needs to have long enough time to measure the channels from all transmit antennas. This is unrealistic in Massive MIMO systems because the channel measurement time grows with the number of antennas, while the channel coherence time is essentially a constant. On the other hand, if CSI is measured at the base station under the TDD mode and based on channel reciprocity, then the base station needs to have enough computing resources to measure the channels between transmit-receive antenna pairs simultaneously, which incurs high hardware costs. Also, the massive antenna arrays need to be carefully calibrated to compensate the reciprocity impairments in practice, which complicates the base station hardware design.

The results of average queue-lengths' growth with respect to $K$ under different values of $B$ are illustrated in Fig. 3. We can see from Fig. 3 that the average queue-lengths increase linearly with respect to $K$ under all $B$ values, agreeing with Lemma 2. Also, the value of $B$ plays an important role in the slope of the linear scaling: the large the $B$ value, the more gradual the slope, again confirming Theorem 1. Also, the slope of $B=64$ is almost the same as that of full CSI.

Next, we study the impacts of $B$ on the congestion control performance and the results are illustrated in Fig. 4. When $B$ is small, we can observe in Fig. 4 that $\mathbf{a}^{\infty}_{B}$ are independent of $K$ and only affected by $B$. The congestion control rates approach that under full CSI as $B$ increases. This confirms the first part of Theorem 2 and Lemma 3. Similar to the growths of queue-length deviations, we can also observe that $B=16$ is the critical point, beyond which the congestion control rates start to exhibit an $O(1/\sqrt{K})$ shrinking gap to $\mathbf{a}^{*}_{B}$. All of these observations agree with the phase transitioning results in Theorem 2.

## V. Conclusion

In this paper, we conducted an in-depth theoretical study on the impact of limited CSI on the performances of the

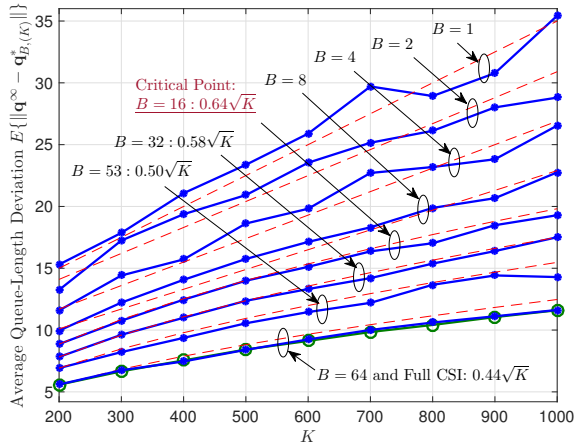


Fig. 2. Average queue-length deviation $\mathbb{E}\{\|\mathbf{q}^{\infty}-\mathbf{q}^{*}_{B,(K)}\|\}$ with respect to $K$ for $B=1,2,4,8,16,32,53,64$.

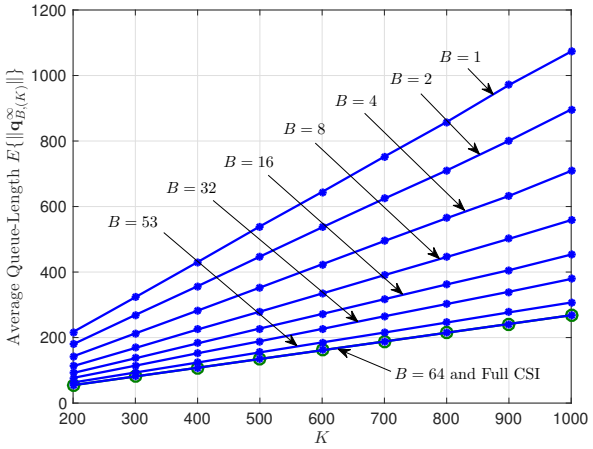


Fig. 3. The growths of average queue-lengths with respect to $K$ for $B=1,2,4,8,16,32,53$, and 64.

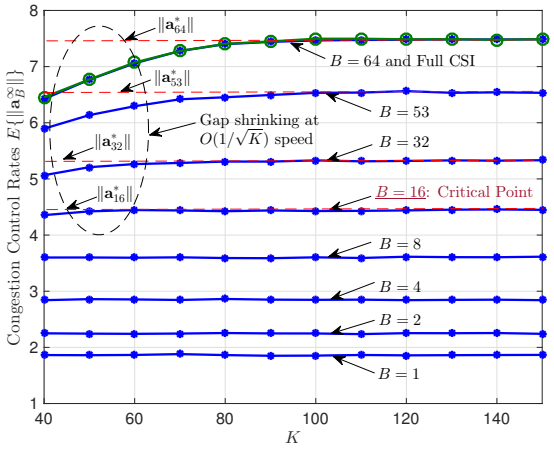


Fig. 4. The steady-state congestion control rates with respect to $K$ for $B=1,2,4,8,16,32,53$, and 64.

queue-length-based joint congestion control and scheduling algorithm in M-MIMO cellular networks. We have theoretically characterized the queueing delay and congestion control scalings under limited CSI. We showed that there exist phase transitioning phenomena in the steady-state queue-length and congestion control rate deviations with respect to CSI quality. Collectively, our theoretical results in this paper advance the understanding of the interactions and trade-offs between delay, throughput, and the accuracy/complexity of CSI acquisition in M-MIMO networks. Our work also establishes a unifying theoretical framework as well as practical design guidelines to enable the development of effective channel quantization schemes for M-MIMO networks. Similar to various known schemes (see, e.g., [27]–[29]) that enhance the original QCS framework for traditional wireless networks under perfect CSI, it is highly interesting to consider new algorithmic techniques to further sharpen the throughput and delay performances for Massive MIMO under imperfect CSI. Also, it is very important to further incorporate user selection/grouping into the MaxWeight scheduling component. To that end, our work serves as an important step toward an exciting M-MIMO networking research paradigm that explores various new congestion control and scheduling algorithmic designs, which could potentially offer better throughput and delay performances under limited CSI.

## Appendix A
## Proof of Lemma 1

For ease of exposition, we first show the second part of Lemma 1. Let $\{p_n[t], n=1,\ldots,N\}$ be an arbitrary feasible power allocation. Since the BS performs MF beam forming by treating $\widehat{\mathbf{H}}[t]$ as if it is the accurate CSI, the received signal can be written as $y_n[t] = s_n[t]p_n[t]\mathbf{h}_n^{\top}[t]\widehat{\mathbf{w}}_n[t] + \sum_{j=1,\neq n}^{N} s_j[t]p_j[t]\mathbf{h}_n^{\top}[t]\widehat{\mathbf{w}}_j[t] + v_n[t]$, where $\widehat{\mathbf{w}}_j[t] = \widehat{\mathbf{h}}_j[t]$, $1\leq j\leq N$, i.e., the $j$-th row of $\widehat{\mathbf{H}}[t]$. Hence, the MF rates $s_{B,n}[t]$ achieved under $\mathbf{H}[t]$ based on the belief that the CSI is $B$-bit CSI $\widehat{\mathbf{H}}[t]$ can be computed as:

$$s_{B,n}[t] = \log_2\left(1+\frac{p_n[t]\left|\mathbf{h}_n^{\dagger}[t]\widehat{\mathbf{h}}_n[t]\right|^2}{N_0+\sum_{j=1,\neq n}^{N}p_j[t]\left|\mathbf{h}_n^{\dagger}[t]\widehat{\mathbf{h}}_j[t]\right|^2}\right)$$
$$< \log_2\left(1+\frac{p_n[t]}{N_0}\left\|\mathbf{h}_n[t]\right\|^2\right) = s_n[t],\ \forall n, \qquad (31)$$

where the inequality in (31) holds because $\left|\mathbf{h}_n^{\dagger}[t]\widehat{\mathbf{h}}_n[t]\right|^2 \leq \|\mathbf{h}_n[t]\|^2$ and $|\mathbf{h}_n^{\dagger}[t]\widehat{\mathbf{h}}_j[t]|^2 \geq 0$. Thus, for every rate point $\mathbf{s}_B[t] = [s_{B,1}[t],\ldots,s_{B,N}[t]]^T \in \mathcal{C}_{\mathbf{H}[t]|\widehat{\mathbf{H}}[t]}$, its corresponding power allocation $\{p_1[t],\ldots,p_N[t]\}$ achieves a rate point $\mathbf{s}[t] = [s_1[t],\ \ldots,s_N[t]]^{\top} \in \mathcal{C}_{\mathbf{H}[t]}$ that dominates $\mathbf{s}_B[t]$ in every coordinate. Hence, $\mathcal{C}_{\widehat{\mathbf{H}}[t]} \subseteq \mathcal{C}_{\mathbf{H}[t]}$. Also, as $B\to\infty$, $\widehat{\mathbf{H}}[t]\to\mathbf{H}[t]$. It thus follows from (31) that $\mathbf{s}_B[t]\uparrow\mathbf{s}[t]$, which implies that $\mathcal{C}_{\widehat{\mathbf{H}}[t]}\to\mathcal{C}_{\mathbf{H}[t]}$.

Next, we argue why the first part of Lemma 1 is true. Let $\mathcal{B}_n^1$ and $\mathcal{B}_n^2$ denote the vector quantization codebooks corresponding to $B_1$ and $B_2$ bits, respectively. Since $B_1\leq B_2$, it follows that the codebook sizes $|\mathcal{B}_n^1|\leq|\mathcal{B}_n^2|$. Hence, given codebook $\mathcal{B}_n^1$, one can construct $\mathcal{B}_n^2$ by simply retaining all codewords in $\mathcal{B}_n^1$ and adding new code words that are not in $\mathcal{B}_n^1$, which implies $\mathcal{B}_n^1\subset\mathcal{B}_n^2$. As a result, for any given CSI $\mathbf{h}_n[t]$, one can always find a codeword in $\mathcal{B}_n^2$ whose distance to $\mathbf{h}_n[t]$ is not larger than that from $\mathcal{B}_n^1$ in the sense of (3). Hence, the SINR term in (31) becomes larger under $\mathcal{B}_n^2$,

implying $s_{B_1,n}[t] \leq s_{B_2,n}[t]$. Since this is true for arbitrary power allocation, we have $\mathcal{C}_{\mathbf{H}[t]|\widehat{\mathbf{H}}_1[t]} \subseteq \mathcal{C}_{\mathbf{H}[t]|\widehat{\mathbf{H}}_2[t]}$.

## APPENDIX B
## PROOF OF LEMMA 2

Dividing $K$ on both sides of (9), we have $\frac{1}{K}\Theta_K(\mathbf{q}_B) = \max_{\mathbf{a},\mathbf{s}_B\in\bar{\mathcal{C}}^B}\left\{\sum_{n=1}^N U_n(a_n) + \sum_{n=1}^N \widehat{q}_{B,n}(s_{B,n}-a_n)\right\}$, where $\widehat{q}_{B,n} = q_{B,n}/K$. Note that the right hand side is precisely $\Theta_1(\mathbf{q}_B)$, for which the maximizer is $\widehat{\mathbf{q}} = \mathbf{q}^*_{B,(1)}$. Hence, we have $\Theta_K(\mathbf{q})$ is maximized at $K\mathbf{q}^*_{B,(1)}$. This proves the first part of Lemma 2.

To show the second part of Lemma 2, we first note from the KKT complementary slackness condition and the monotonicity of $U_n(\cdot)$ that, at optimality, $a^*_n = s^*_{B,n}, \forall n$. We let $a^*_n(B_1)$ and $a^*_n(B_2)$ denote the optimal congestion control rates under $B_1$ and $B_2$, respectively. If $B_1 \leq B_2$, we have from Lemma 1 that $s^*_{B_1,n} \leq s^*_{B_2,n}$, which further implies $a^*_n(B_1) \leq a^*_n(B_2)$. On the other hand, from the KKT stationarity condition, we have $U_n'(a^*_n(B)) - q^*_{(B),n} = 0$. Since $a^*_n(B_1) \leq a^*_n(B_2)$, it follows from the concavity of $U_n(\cdot)$ that $q^*_{(B_1),n} \geq q^*_{(B_2),n}$. This completes the proof.

## APPENDIX C
## PROOF OF THEOREM 3

Consider the quadratic Lyapunov function defined in Theorem 3: $V(\mathbf{q}[t]) = \frac{1}{2K}\|\mathbf{q}[t] - \mathbf{q}^*_{B,(K)}\|^2$, where $\mathbf{q}[t]$ represents the queue-length vector in time-slot $t$ under parameters $K$ and $B$; and $\mathbf{q}^*_{B,(K)}$ denotes the optimal dual solution for the static version of Problem JCCR under parameter $K$. Then, the one-slot mean Lyapunov drift of $V_K(\mathbf{q}[t])$, which can computed as:

$$\begin{aligned}
&\mathbb{E}\{V(\mathbf{q}[t+1]) - V(\mathbf{q}[t])|\mathbf{q}[t]\}\\
&= \frac{1}{2K}\mathbb{E}\left\{(\mathbf{q}[t+1]-\mathbf{q}[t])^\top(\mathbf{q}[t+1]+\mathbf{q}[t]-2\mathbf{q}^*_{B,(K)})\Big|\mathbf{q}[t]\right\}\\
&\overset{(a)}{\leq} \frac{1}{2K}\mathbb{E}\left\{(-\mathbf{s}_B[t]+\mathbf{a}[t])^\top(2\mathbf{q}[t]-2\mathbf{q}^*_{B,(K)}-\mathbf{s}_B[t]+\mathbf{a}[t])\Big|\mathbf{q}[t]\right\}\\
&= \frac{1}{K}(\mathbf{q}[t]-\mathbf{q}^*_{B,(K)})^\top(-\mathbf{s}_B[t]+\mathbf{a}[t]) + \frac{1}{2K}\mathbb{E}\left\{\|-\mathbf{s}_B[t]+\mathbf{a}[t]\|^2\right\},
\end{aligned}$$

where $(a)$ follows from the non-expansive property of the $\max\{0,\cdot\}$ operation. Note that, from the definition of Algorithm 1, we have $\mathbb{E}\{\|\mathbf{a}[t]\|^2|\mathbf{q}[t]\} < A_2^{\max}N$. Also, since $s_{B,n}[t]$ falls in a bounded instantaneous capacity region $\mathcal{C}_{\widehat{\mathbf{H}}[t]}$, $\forall n$, we must have $s_{B,n}[t] \leq s^{\max}$ for some $s^{\max} > 0$. Hence, by defining $D_0 \triangleq \frac{N}{2}(A_2^{\max} + (s^{\max})^2)$, which is a constant upper bound of the second moments of the arrival and service processes, we have

$$\begin{aligned}
&\mathbb{E}\left\{\Delta V(\mathbf{q}[t])|\mathbf{q}[t]\right\} \leq \frac{1}{K}(\mathbf{q}[t]-\mathbf{q}^*_{B,(K)})^\top\mathbb{E}\left\{\mathbf{a}[t]-\mathbf{s}_B[t]\right\} + \frac{D_0}{K}\\
&\overset{(a)}{=} \frac{1}{K}(\mathbf{q}[t]-\mathbf{q}^*_{B,(K)})^\top(\mathbb{E}\{\mathbf{a}[t]|\mathbf{q}[t]\}-\mathbf{s}^*_B) +\\
&\quad \frac{1}{K}\mathbb{E}\{(\mathbf{q}[t]-\mathbf{q}^*_{B,(K)})^\top(\mathbf{s}^*_B-\mathbf{s}_B[t])|\mathbf{q}[t]\} + \frac{D_0}{K},\\
&\overset{(b)}{\leq} \frac{1}{K}(\mathbf{q}[t]-\mathbf{q}^*_{B,(K)})^\top(\mathbb{E}\{\mathbf{a}[t]|\mathbf{q}[t]\}-\mathbf{s}^*_B) +\\
&\quad \frac{1}{K}\|\mathbf{q}[t]-\mathbf{q}^*_{B,(K)})^\top\| \times \mathbb{E}\{\|\mathbf{s}^*_B-\mathbf{s}_B[t]\||\mathbf{q}[t]\} + \frac{D_0}{K},
\end{aligned} \tag{32}$$

where $\mathbf{s}^*_B$ is such that $(\mathbf{s}^*_B, \mathbf{q}^*_{B,(K)})$ is a pair of optimal primal and dual solutions to Problem $K$-DJCCS under parameter $K$. In (32), $(a)$ follows from adding and subtracting $\mathbf{s}^*_B$ as well as the fact that $\mathbf{a}[t]$ is independent of the channel state and determined solely by $\mathbf{q}[t]$; and $(b)$ follows from Cauchy-Schwarz inequality.

Note from Lemma 3 that $\mathbf{s}^*_B$ is independent of $K$ and $s_{B,n}[t] \in \mathcal{C}_{\widehat{\mathbf{H}}[t]}$ is upper-bounded. Thus, we have

$$\mathbb{E}\{\|\mathbf{s}^*_B - \mathbf{s}_B[t]\||\mathbf{q}[t]\} \leq D_{(B)} \triangleq \max_{\mathbf{q}:\|\mathbf{q}\|=1}\mathbb{E}\{\|\mathbf{s}^*_B-\mathbf{s}_B\|\mathbf{q}\}, \tag{33}$$

where $D_{(B)}$ is a constant depending only on the CSI accuracy $B$ and independent of $K$, which bounds the cross term in (32). Hence, we can further upper bound (32) as:

$$\begin{aligned}
\mathbb{E}\left\{\Delta V(\mathbf{q}[t])|\mathbf{q}[t]\right\} \leq \frac{1}{K}(\mathbf{q}[t]-\mathbf{q}^*_{B,(K)})^\top(\mathbb{E}\{\mathbf{a}[t]|\mathbf{q}[t]\}-\mathbf{s}^*_B) +\\
\frac{1}{K}\|\mathbf{q}[t]-\mathbf{q}^*_{B,(K)})^\top\|D_{(B)} + \frac{D_0}{K},
\end{aligned} \tag{34}$$

Now, let us consider the first term on the right hand side in (34), i.e., $\frac{1}{K}(\mathbf{q}[t]-\mathbf{q}^*_{B,(K)})^\top(\mathbb{E}\{\mathbf{a}[t]|\mathbf{q}[t]\}-\mathbf{s}^*)$. Since $U_n(\cdot)$ is concave and increasing, $\forall n$, we have

$$\left(q_n[t]-q^*_{B,(K),n}\right)^\top\left[U_n'^{-1}\left(\frac{q_n[t]}{K}\right) - U_n'^{-1}\left(\frac{q^*_{B,(K),n}}{K}\right)\right] \leq 0.$$

Thus, by Cauchy-Schwatz inequality, we have:

$$\begin{aligned}
&(\mathbf{q}[t]-\mathbf{q}^*_{B,(K)})^\top(\mathbb{E}\{\mathbf{a}[t]|\mathbf{q}[t]\}-\mathbf{s}^*_B) = \sum_{n=1}^N\left(q_n[t]-q^*_{B,(K),n}\right)^\top\\
&\times\left[U_n'^{-1}\left(\frac{q_n[t]}{K}\right) - U_n'^{-1}\left(\frac{q^*_{B,(K),n}}{K}\right)\right] \leq -\sum_{n=1}^N\left|q_n[t]-\right.\\
&\quad\left.q^*_{B,(K),n}\right|\left|U_n'^{-1}\left(\frac{q_n[t]}{K}\right)-U_n'^{-1}\left(\frac{q^*_{B,(K),n}}{K}\right)\right|.
\end{aligned} \tag{35}$$

By the strong convexity of $-U_n(\cdot)$ and the Lipschitz continuity of $U_n'(\cdot)$, we have

$$\left|U_n'\left(a_{n,1}\right) - U_n'\left(a_{n,2}\right)\right| \leq \Phi\left|a_{n,1}-a_{n,2}\right|.$$

Therefore, by the inverse function lemma, we have

$$\frac{1}{\Phi}\left|\frac{q_n[t]}{K}-\frac{q^*_{B,(K),n}}{K}\right| \leq \left|U_n'^{-1}\left(\frac{q_n[t]}{K}\right)-U_n'^{-1}\left(\frac{q^*_{B,(K),n}}{K}\right)\right|.$$

Hence, we can further upper-bound (35) as:

$$\begin{aligned}
(\mathbf{q}[t]-\mathbf{q}^*_{B,(K)})^\top(\mathbb{E}\{\mathbf{a}[t]|\mathbf{q}[t]\}-\mathbf{s}^*_B) \leq -\frac{1}{\Phi K}\sum_{n=1}^N\left(q_n[t]-\right.\\
\left.q^*_{B,(K),n}\right)^2 = -\frac{1}{\Phi K}\left\|\mathbf{q}[t]-\mathbf{q}^*_{B,(K)}\right\|^2.
\end{aligned} \tag{36}$$

Substituting (36) into (34), we have

$$\begin{aligned}
\mathbb{E}\left\{\Delta V(\mathbf{q}[t])|\mathbf{q}[t]\right\} \leq -\frac{1}{\Phi K^2}\left\|\mathbf{q}[t]-\mathbf{q}^*_{B,(K)}\right\|^2 +\\
\frac{1}{K}\|\mathbf{q}[t]-\mathbf{q}^*_{B,(K)})^\top\|D_{(B)} + \frac{D_0}{K}.
\end{aligned} \tag{37}$$

Now, suppose that $\left\|\mathbf{q}[t]-\mathbf{q}^*_{B,(K)}\right\| \geq \beta_1 K$, where $\beta_1$ will

be specified shortly. Note also that $K \geq 1$, we have

$$\frac{1}{\|\mathbf{q}[t]-\mathbf{q}^*_{B,(K)}\|} \leq \frac{1}{\beta_1 K} \leq \frac{1}{\beta_1}.$$

It then follows that (37) can be further upper bounded as:

$$\begin{aligned}\mathbb{E}\{\Delta V(\mathbf{q}[t])|\mathbf{q}[t]\} &= -\frac{1}{\Phi K}\big\|\mathbf{q}[t]-\mathbf{q}^*_{B,(K)}\big\| \cdot \frac{\big\|\mathbf{q}[t]-\mathbf{q}^*_{B,(K)}\big\|}{K} \\ &+\frac{1}{K}\|\mathbf{q}[t]-\mathbf{q}^*_{B,(K)})^\top\|D_{(B)}+\big\|\mathbf{q}[t]-\mathbf{q}^*_{B,(K)}\big\|\frac{D_0}{\big\|\mathbf{q}[t]-\mathbf{q}^*_{B,(K)}\big\|K} \\ &\leq -\frac{1}{\Phi K}\big\|\mathbf{q}[t]-\mathbf{q}^*_{B,(K)}\big\|\Big(\beta_1 - D_{(B)}\Phi - \frac{D_0\Phi}{\beta_1}\Big). \qquad (38)\end{aligned}$$

By choosing $\beta_1$ such that $\beta_1 - D_1\Phi - \frac{D_0\Phi}{\beta_1} > 0$, we have

$$\mathbb{E}\{\Delta V(\mathbf{q}[t])|\mathbf{q}[t]\} \leq -\frac{\hat{\delta_1}}{\Phi K}\big\|\mathbf{q}[t]-\mathbf{q}^*_{B,(K)}\big\| \qquad (39)$$

where $\hat{\delta_1} = \beta_1 - D_{(B)}\Phi - \frac{D_0\Phi}{\beta_1}$. Solving $\beta_1 - D_{(B)}\Phi - \frac{D_0\Phi}{\beta_1} = 0$ and plugging in the obtained $\beta_1$ to define a ball $\mathcal{B}_1 \triangleq \{\mathbf{q} : \big\|\mathbf{q}-\mathbf{q}^*_{B,(K)}\big\| \leq \frac{K}{2}[(D_{(B)}\Phi) + \sqrt{(D_{(B)}\Phi)^2 + 4D_0\Phi}]\}$, we have

$$\mathbb{E}\{\Delta V(\mathbf{q}[t])|\mathbf{q}[t]\} \leq -\frac{\delta_1}{K}\big\|\mathbf{q}[t]-\mathbf{q}^*_{B,(K)}\big\|, \text{ if } \mathbf{q}[t] \in \mathcal{B}_1^c, \qquad (40)$$

where $\delta_1 \triangleq \frac{\hat{\delta_1}}{\Phi}$. On the other hand, when $\mathbf{q}[t] \in \mathcal{B}_1$, it is clearly true that $\mathbb{E}\{\Delta V(\mathbf{q}[t])|\mathbf{q}[t]\} \leq \eta_1$ for some $\eta_1 > 0$. Combining these facts yields the following:

$$\mathbb{E}\{\Delta V(\mathbf{q}[t])|\mathbf{q}[t]=\mathbf{q}\} \leq -\frac{\delta_1}{K}\|\mathbf{q}-\mathbf{q}^*_{B,(K)}\|\mathbb{1}_{\mathcal{B}_1^c}(\mathbf{q}) + \eta_1 \mathbb{1}_{\mathcal{B}_1}(\mathbf{q}).$$

This completes the proof of Theorem 3.

## REFERENCES


[1] E. G. Larsson, O. Edfors, and T. L. Marzetta, "Massive MIMO for next generation wireless systems," *IEEE Commun. Mag.*, vol. 52, no. 2, pp. 186–195, Feb. 2014.

[2] F. Rusek, D. Persson, B. K. Lau, E. G. Larsson, T. L. Marzetta, O. Edfors, and F. Tufvesson, "Scaling up MIMO: Opportunities and challenges with very large arrays," *IEEE Signal Process. Mag.*, vol. 30, no. 1, pp. 40–46, Jan. 2013.

[3] L. Lu, G. Y. Li, A. L. Swindlehurst, A. Ashikhmin, and R. Zhang, "An overview of massive MIMO: Benefits and challenges," *IEEE Journal of Selected Topics in Signal Processing*, vol. 8, no. 5, pp. 742–758, Oct. 2014.

[4] Argos: Practical many-antenna base stations. [Online]. Available: argos.rice.edu

[5] E. G. Larsson and F. Tufvesson, "Massive MIMO systems tutorial," 2013. [Online]. Available: http://www.commsys.isy.liu.se/vlm/icc_tutorial_P2.pdf

[6] X. Lin and N. B. Shroff, "The impact of imperfect scheduling on cross-layer congestion control in wireless networks," *IEEE/ACM Trans. Netw.*, vol. 14, no. 2, pp. 302–315, Apr. 2006.

[7] A. Eryilmaz and R. Srikant, "Joint congestion control, routing, and MAC for stability and fairness in wireless networks," *IEEE J. Sel. Areas Commun.*, vol. 24, no. 8, pp. 1514–1524, Aug. 2006.

[8] M. J. Neely, E. Modiano, and C.-P. Li, "Fairness and optimal stochastic control for heterogeneous networks," *IEEE/ACM Trans. Netw.*, vol. 16, no. 2, pp. 396–409, Apr. 2008.

[9] A. Eryilmaz and R. Srikant, "Fair resource allocation in wireless networks using queue-length-based scheduling and congestion control," *IEEE/ACM Trans. Netw.*, vol. 15, no. 6, pp. 1333–1344, Dec. 2007.

[10] X. Lin, N. B. Shroff, and R. Srikant, "A tutorial on cross-layer optimization in wireless networks," *IEEE J. Sel. Areas Commun.*, vol. 24, no. 8, pp. 1452–1463, Aug. 2006.

[11] C. Shepard, H. Yu, N. Anand, L. E. Li, T. L. Marzetta, R. Yang, and L. Zhong, "Argos: Practical many-antenna base stations," in *Proc. ACM MobiCom*, Istanbul, Turkey, August 2012, pp. 53–64.

[12] A. Eryilmaz and R. Srikant, "Fair resource allocation in wireless networks using queue-length-based scheduling and congestion control," in *Proc. IEEE INFOCOM*, Miami, FL, Mar. 2005, pp. 1804–1814.

[13] H. Weingarten, Y. Steinberg, and S. Shamai (Shitz), "The capacity region of the Gaussian multiple-input multiple-output broadcast channel," *IEEE Trans. Inf. Theory*, vol. 52, no. 9, pp. 3936–3964, Sep. 2006.

[14] N. Jindal, "MIMO broadcast channels with finite rate feedback," *IEEE Trans. Inf. Theory*, vol. 52, no. 11, pp. 5045–5059, Nov. 2006.

[15] W. Santipach and M. Honig, "Signature optimiation for CDMA with limited feedback," *IEEE Trans. Inf. Theory*, vol. 51, no. 10, pp. 3475–3492, Oct. 2005.

[16] W. Santipach and M. L. Honig, "Asymptotic performance of MIMO wireless channels with limited feedback," in *Proc. IEEE Mil. Commun. Conf.*, vol. 1, Oct. 2003, pp. 141–146.

[17] ——, "Asymptotic capacity of beamforming with limited feedback," in *Proc. IEEE ISIT*, Jul. 2004, p. 290.

[18] C. K. Au-Yeung and D. J. Love, "On the performance of random vector quantization limited feedback beamforming in a MISO system," *IEEE Trans. Wireless Commun.*, vol. 6, no. 2, pp. 458–462, Feb. 2007.

[19] A. F. Molisch, V. V. Ratnam, S. Han, Z. Li, S. L. H. Nguyen, L. Li, and K. Haneda, "Hybrid Beamforming for Massive MIMO – A Survey," *arXiv preprint arXiv:1609.05078*, 2016.

[20] J. Y. A. A. Adhikary, J. Nam and G. Caire, "Joint spatial division and multiplexing – the large-scale array regime," *IEEE Trans. Inf. Theory*, vol. 59, no. 10, pp. 6441 – 6463, Oct. 2013.

[21] C. Joo, X. Lin, J. Ryu, and N. B. Shroff, "Distributed greedy approximation to maximum weighted independent set for scheduling with fading channels," *IEEE/ACM Transactions on Networking*, vol. 24, no. 3, pp. 1476 – 1488, June 2016.

[22] B. Ji, G. R. Gupta, M. Sharma, X. Lin, and N. B. Shroff, "Achieving optimal throughput and near-optimal asymptotic delay performance in multi-channel wireless networks with low complexity: A practical greedy scheduling policy," *IEEE/ACM Transactions on Networking*, vol. 23, no. 3, pp. 880 – 893, June 2015.

[23] C. Joo and N. B. Shroff, "Local greedy approximation for scheduling in multi-hop wireless networks," *IEEE Transaction on Mobile Computing*, vol. 11, no. 3, pp. 414 – 426, March 2012.

[24] D. Bethanabhotla, G. Caire, and M. J. Neely, "WiFlix: Adaptive video streaming in massive MU-MIMO wireless networks," *IEEE Trans. Wireless Commun.*, vol. 15, no. 6, pp. 4088–4103, Jun. 2016.

[25] M. S. Bazaraa, H. D. Sherali, and C. M. Shetty, *Nonlinear Programming: Theory and Algorithms*, 3rd ed. New York, NY: John Wiley & Sons Inc., 2006.

[26] S. P. Meyn and R. L. Tweedie, *Markov Chains and Stochastic Stability*, 2nd ed. Cambridge, UK: Cambridge University Press, 2009.

[27] J. Liu, A. Eryilmaz, N. B. Shroff, and E. Bentley, "Heavy-ball: A new approach to tame delay and convergence in wireless network optimization," in *Proc. IEEE INFOCOM*, April 10-15, 2016.

[28] M. J. Neely, "Super-fast delay tradeoffs for utility optimal fair scheduling in wireless networks," *IEEE J. Sel. Areas Commun.*, vol. 24, no. 8, pp. 1489–1501, Aug. 2006.

[29] L. Huang and M. J. Neely, "Delay reduction via lagrange multipliers in stochastic network optimization," *IEEE Trans. Autom. Control*, vol. 56, no. 4, pp. 842–857, Apr. 2011.

**Jia Liu** (S'03–M'10–SM'16) received his Ph.D. degree in the Bradley Department of Electrical and Computer Engineering at Virginia Tech, Blacksburg, VA in 2010. He joined the Ohio State University as a postdoctoral researcher afterwards. He is currently a Research Assistant Professor in the Department of Electrical and Computer Engineering at the Ohio State University. His research focus is in the areas of optimization of communication systems and networks, theoretical foundations of cross-layer optimization on wireless networks, design of algorithms, and information theory. Dr. Liu is a senior member of IEEE. His work has received numerous awards at top venues, including IEEE INFOCOM 2016 Best Paper Award, IEEE INFOCOM 2013 Best Paper Runner-up Award, IEEE INFOCOM 2011 Best Paper Runner-up Award, and IEEE ICC 2008 Best Paper Award. He is a recipient of the Bell Labs President Gold Award in 2001 and Chinese Government Award for Outstanding Ph.D. Students Abroad in 2008. He has served as a TPC member for IEEE INFOCOM since 2010.

**Atilla Eryilmaz** (S'00–M'06–SM'17) received his M.S. and Ph.D. degrees in Electrical and Computer Engineering from the University of Illinois at Urbana-Champaign in 2001 and 2005, respectively. Between 2005 and 2007, he worked as a Postdoctoral Associate at the Laboratory for Information and Decision Systems at the Massachusetts Institute of Technology. He is currently an Associate Professor of Electrical and Computer Engineering at The Ohio State University. Dr. Eryilmaz's research interests include design and analysis for communication networks, optimal control of stochastic networks, optimization theory, distributed algorithms, pricing in networked systems, and information theory. He received the NSF-CAREER Award in 2010 and two Lumley Research Awards for Research Excellence in 2010 and 2015. He is a co-author of the 2012 IEEE WiOpt Conference Best Student Paper, the 2016 IEEE Infocom Best Paper, and 2017 IEEE WiOpt Conference Best Paper. He has served as TPC co-chair of IEEE WiOpt in 2014 and of ACM Mobihoc in 2017, and is an Associate Editor of IEEE/ACM Transactions on Networking since 2015, and of IEEE Transactions on Network Science and Engineering since 2017.

**Ness B. Shroff** (S'91–M'93–SM'01–F'07) received his Ph.D. degree in Electrical Engineering from Columbia University in 1994. He joined Purdue university immediately thereafter as an Assistant Professor in the school of ECE. At Purdue, he became Full Professor of ECE in 2003 and director of CWSA in 2004, a university-wide center on wireless systems and applications. In July 2007, he joined The Ohio State University, where he holds the Ohio Eminent Scholar endowed chair in Networking and Communications, in the departments of ECE and CSE. He holds or has held visiting (chaired) professor positions at Tsinghua University, Beijing, China, Shanghai Jiaotong University, Shanghai, China, and the Indian Institute of Technology, Bombay, India. Dr. Shroff is currently an editor at large of IEEE/ACM Trans. on Networking, senior editor of IEEE Transactions on Control of Networked Systems, and technical editor for the IEEE Network Magazine. He has received numerous best paper awards for his research and listed Thomson Reuters Book on The World's Most Influential Scientific Minds as well as noted as a highly cited researcher by Thomson Reuters. He also received the IEEE INFOCOM achievement award for seminal contributions to scheduling and resource allocation in wireless networks.

**Elizabeth S. Bentley** has a B.S. degree in Electrical Engineering from Cornell University, a M.S. degree in Electrical Engineering from Lehigh University, and a Ph.D. degree in Electrical Engineering from University at Buffalo. She was a National Research Council Post-Doctoral Research Associate at the Air Force Research Laboratory in Rome, NY. Currently, she is employed by the Air Force Research Laboratory in Rome, NY, performing in-house research and development in the Networking Technology branch. Her research interests are in cross-layer optimization, wireless multiple-access communications, wireless video transmission, modeling and simulation, and directional antennas/directional networking.